Geochronology, Nd isotopes and reconnaissance geochemistry of volcanic and metavolcanic rocks of the São Luís Craton, northern Brazil: Implications for tectonic setting and crustal evolution

Evandro L. Klein [a,*], Renê Luzardo [b], Candido A.V. Moura [c], Denise C. Lobato [a], Reinaldo S.C. Brito [d], Richard Armstrong [e]

[a] CPRM/Geological Survey of Brazil, Av. Dr. Freitas, 3645, Belém-PA, CEP: 66095-110, Brazil
[b] CPRM/Geological Survey of Brazil, Av. André Araújo, 2160, Manaus-AM, CEP: 69060-001, Brazil
[c] Universidade Federal do Pará, Centro de Geociências, CP 1611, Belém-PA, CEP: 66075-900, Brazil
[d] CPRM/Geological Survey of Brazil, SGAN Quadra 603, Módulo J, Parte A, 1° andar, Brasília-DF, CEP: 70830-030, Brazil
[e] Research School of Earth Sciences, Mills Road, The Australian National University, Canberra 0200, Australia

ARTICLE INFO

ABSTRACT

New field work, in addition to zircon geochronology, Nd isotopes and reconnaissance geochemical data allow the recognition of Paleoproterozoic volcanic and metavolcanic sequences in the São Luís Craton of northern Brazil. These sequences record at least five volcanic pulses occurring probably in three distinct epochs and in different tectonic settings. (1) The Pirocaua Formation of the Aurizona Group comprises early arc-related calc-alkaline metapyroclastic rocks of 2240 ± 5 Ma formed from juvenile protoliths in addition to minor older crustal components. (2) The Matará Formation of the Aurizona Group holds mafic tholeiitic and ultramafic metavolcanic rocks of back arc and/or island arc setting, which are likely coeval to the Pirocaua Formation. (3) The Serra do Jacaré volcanic unit is composed of tholeiitic basalts and predominantly metaluminous, normal- to high-K calc-alkaline andesites of 2164 ± 3 Ma formed in mature arc or active continental margin from juvenile protoliths along with subordinate older (Paleoproterozoic) materials and associated to the main calc-alkaline orogenic stage. (4) The Rio Diamante Formation consists of late-orogenic metaluminous, medium-K, calc-alkaline rhyolite to dacite and tuffs of 2160 ± 8 Ma formed in continental margin setting from reworked Paleoproterozoic crust (island arc) with incipient Archean contribution. (5) The Rosilha volcanic unit is composed of weakly peraluminous, medium-K, calc-alkaline dacite and tuff formed probably at about 2068 Ma from reworked crustal protoliths. As a whole the volcanic and metavolcanic rocks record and characterized better the previously proposed orogenic evolution of the São Luís Craton.

© 2008 Elsevier Ltd. All rights reserved.

1. Introduction

Current interpretations consider the São Luís Craton in northern Brazil (Fig. 1) as part of a major Paleoproterozoic (Rhyacian) orogen that comprises also the West African Craton (Klein and Moura, 2008). The lithology of the São Luís Craton is described as composed mainly of a metavolcano-sedimentary sequence and few generations of granitoids (Klein et al., 2005a and references therein). The existence of volcanic and metavolcanic rocks in this craton is reported at least since the work of Costa et al. (1977). However, these rocks have neither been characterized nor separated in the regional maps as individual units, being rather included either in a plutono-volcanic suite or in a metavolcano-sedimentary se-

quence (Costa et al., 1977; Abreu et al., 1980; Pastana, 1995; Klein and Moura, 2001; Klein et al., 2005a). Klein and Moura (2001) reported zircon geochronology for a metapyroclastic rock belonging to the metavolcano-sedimentary sequence (Aurizona Group) that yielded an age of 2240 ± 5 Ma. Klein et al. (2005a) published Nd isotope data from a metadacite (Aurizona Group) and a dacite (undivided unit), with T_{DM} model ages of 2.48 and 2.42 Ga, respectively. These crystallization and model ages are quite distinct from those of the main period of magmatism in the São Luís Craton, which is represented by the voluminous juvenile, calc-alkaline magmatism of 2168–2147 Ma with T_{DM} ages of 2.22–2.26 Ga (Klein and Moura, 2001, 2003; Klein et al., 2005a).

In recent semi-detail geological mapping undertaken by the Geological Survey of Brazil in the central portion of the São Luís Craton (Klein et al., in press), a series of supracrustal rocks have been individualized (Fig. 2). Although some of these rock units are volumetrically subordinate, their characterization bears impor-

---
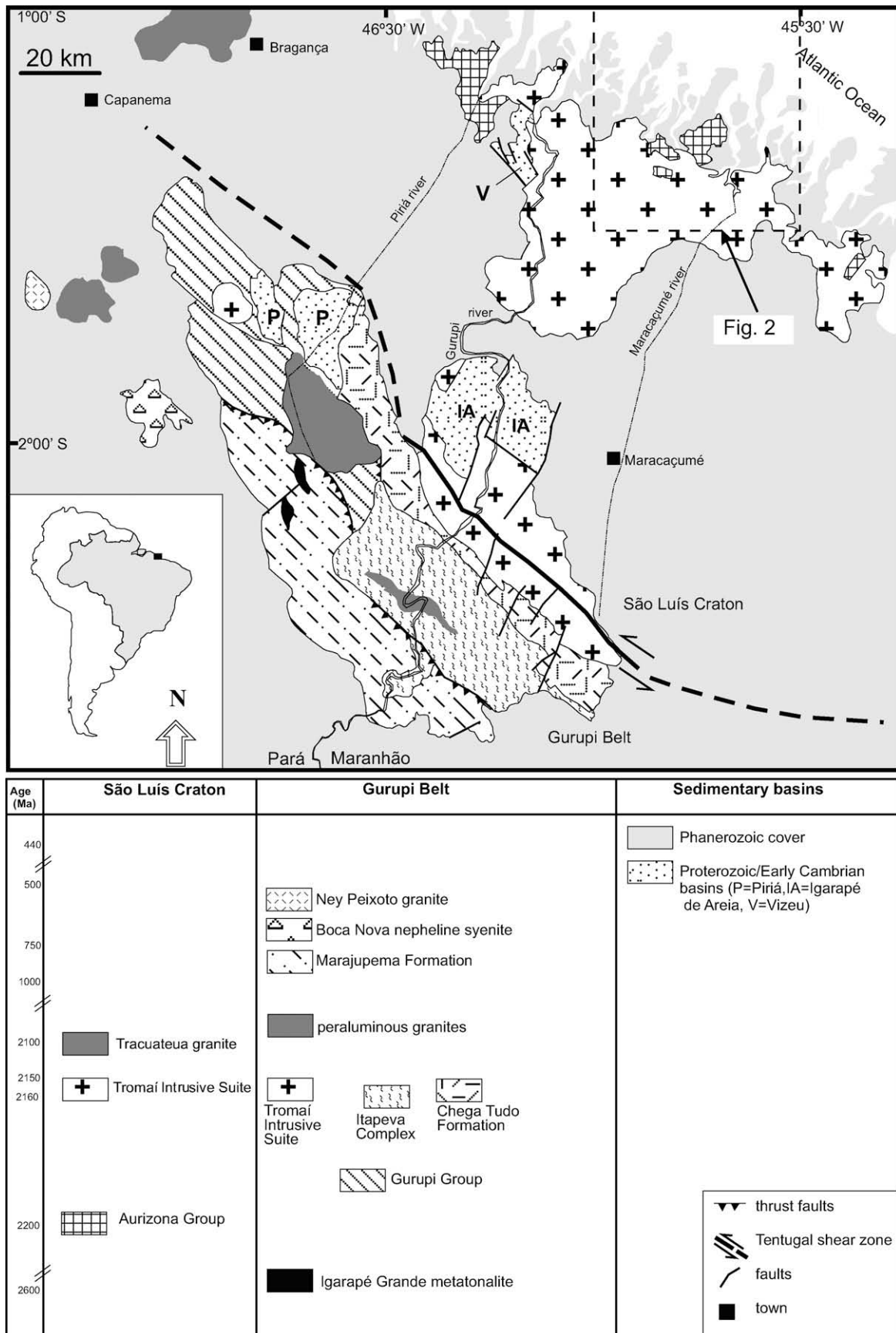
Fig. 1. Geologic map of the São Luís Craton and Gurupi belt and location of the study area (arrow).

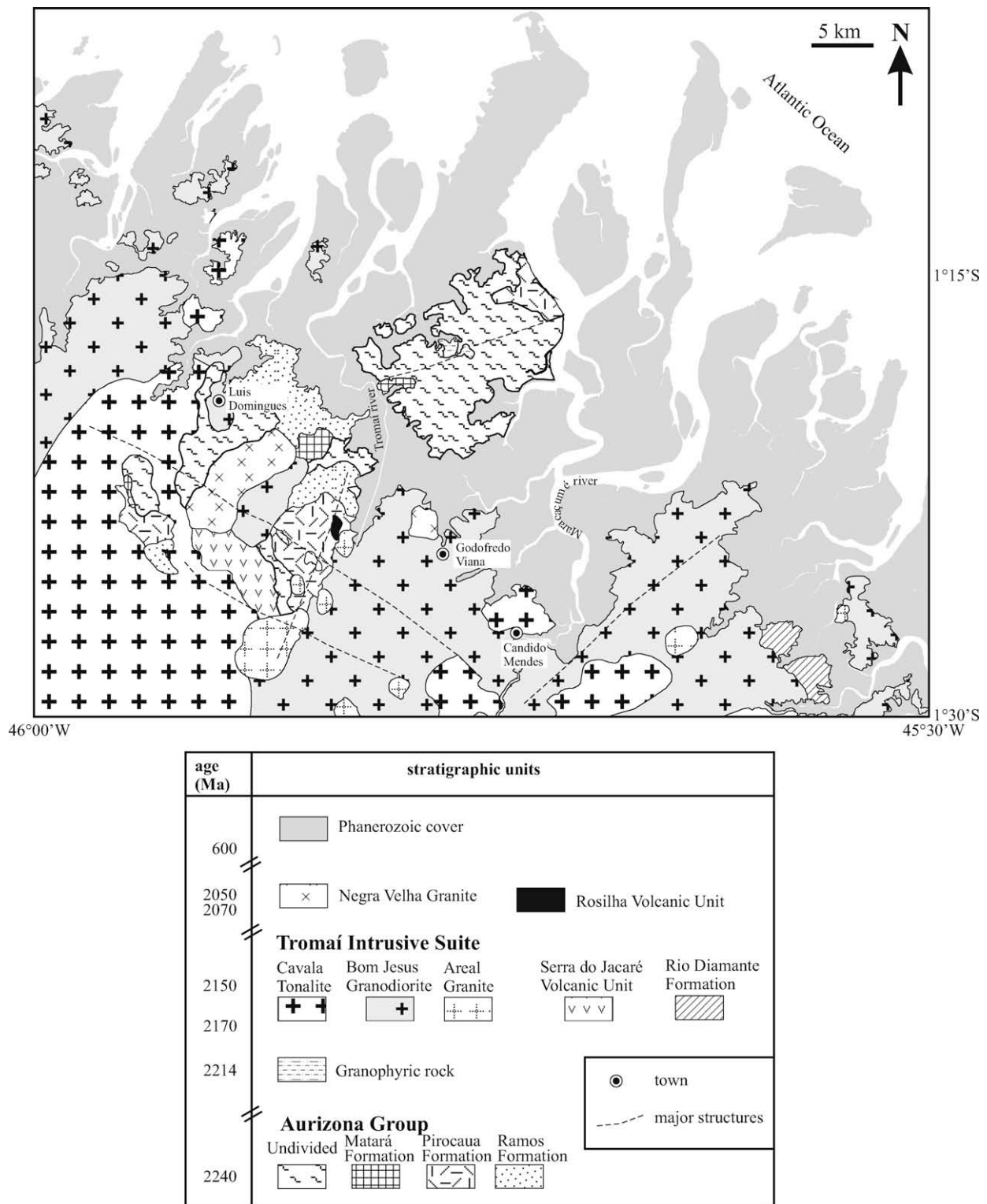| age (Ma)	stratigraphic units		
600	Phanerozoic cover		
2050 / 2070	Negra Velha Granite (×)		Rosilha Volcanic Unit
	Tromaí Intrusive Suite		
2150	Cavala Tonalite (+ +)	Bom Jesus Granodiorite (+)	Areal Granite
2170		Serra do Jacaré Volcanic Unit (v v v)	Rio Diamante Formation
2214	Granophyric rock		town (⊙)
	Aurizona Group		major structures (- - -)
2240	Undivided	Matará Formation	Pirocaua Formation	Ramos Formation

Fig. 2. Geologic map of the study area in the central portion of the São Luís Craton (adapted from Klein et al., in press).

tant constraints for both the stratigraphy and geological evolution of the cratonic area. In this paper, we present a petrographic and preliminary geochemical assessment of these newly-described units, in addition to new geochronological and Nd isotope data. The results allow us to discuss aspects such as magma genesis, the tectonic setting in which the rocks have formed, and the implications for the crustal evolution of the São Luís Craton.

2. Geologic setting

The São Luís Craton is composed of subduction-related calc-alkaline granitoids, represented by the Tromaí Intrusive Suite of 2165–2149 Ma (Klein and Moura, 2001, 2003; Klein et al., 2005a), and of younger crust-derived, peraluminous granites of the Tracuateua Intrusive Suite, dated at 2086 ± 10 Ma (Palheta,
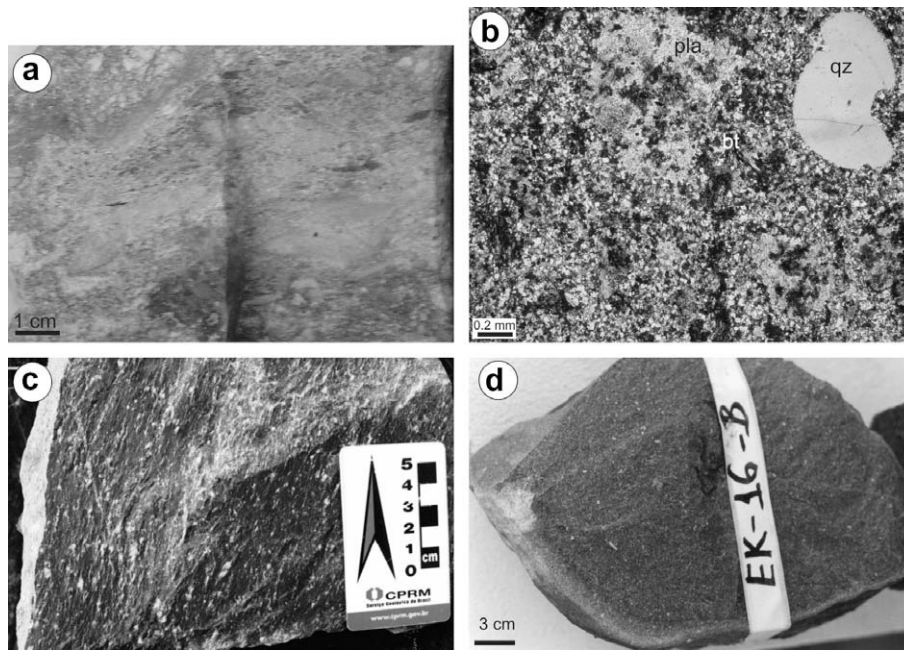
Fig. 3. (a) photograph of a hand sample of a foliated volcanic agglomerate of the Pirocaua Formation; (b) photomicrograph of an andesite of the Serra do Jacaré volcanic unit showing corroded quartz (qz) and altered plagioclase (pla) phenocrysts set in a biotite-rich (bt) matrix; (c) hand sample photograph of a dacite porphyry of the Rio Diamante Formation; (d) hand sample photograph of a dacite of the Rosilha volcanic unit.

2001) (Fig. 1). Both the calc-alkaline and the peraluminous granitoids are massive to foliated and underwent very low-grade metamorphism/hydrothermal alteration at regional scale, but the primary igneous mineralogy and textures are largely preserved. The granitoids intruded the metavolcano-sedimentary sequence of the Aurizona Group of 2240 Ma (Klein and Moura, 2001), which is composed of schists of variable compositions, metavolcanic and metapyroclastic rocks, quartzites and subordinated amphibolites. All rocks underwent greenschist (±lower amphibolite) facies metamorphism and most of the rocks show a penetrative schistosity and local folding. Klein et al. (in press) subdivided the Aurizona Group into three formations: Matará (basic and ultrabasic rocks); Pirocaua (metavolcanic and metapyroclastic rocks, schists); Ramos (quartzite, phyllite, schists). Those authors also described three volcanic sequences (Serra do Jacaré, Rio Diamante, and Rosilha) that are composed of unmetamorphosed and mostly undeformed flows and tuffs. These volcanic sequences occur mostly as subordinate bodies (Fig. 2).

The cratonic rocks have not been affected by any other thermal event after about 1900 Ma, according to Rb–Sr and K–Ar evidence (Klein and Moura, 2001 and references therein). The São Luís Craton has been interpreted as part of a Paleoproterozoic accretionary orogen, with the juvenile calc-alkaline granitoids and the supracrustal rocks formed in intra-oceanic settings, whereas the peraluminous granites record the collision phase of the orogen, which is better represented in the basement of the adjoining Gurupi Belt (Klein et al., 2005a,b).

3. Characteristics of the volcanic successions

3.1. Pirocaua Formation

The Pirocaua Formation groups metamorphosed felsic pyroclastic and volcanic rocks. These vary from very fine- to coarse-grained rocks and comprise tuff of rhyolitic composition, cineritic tuff, volcanic agglomerate, rhyolite, and dacite. Some very fine-grained and altered rocks of difficult classification were termed generally felsite and/or felsic metavolcanic/metavolcanoclastic rocks. All samples show predominantly grey color and bear a well-developed foliation.

In felsites and metavolcanoclastic rocks, only domains comprising poly-crystalline aggregates of anhedral quartz grains set in a matrix composed of K-feldspar-quartz intergrowths are recognized under the microscope. In places, the matrix contains also opaque minerals, sericite and apatite.

The volcanic agglomerates are deformed rocks with a well-developed foliation (Fig. 3a). Stretched/elongated quartz porphyroclasts and poly-crystalline aggregates of quartz and/or quartz–chalcedony–plagioclase, rounded fragments of quartz phenocrysts, and fragments of volcanic rocks occur in a fine-grained quartzo–feldspathic matrix and are elongated parallel to the foliation. Fine seams of sericite, opaque minerals, and dark carbonaceous matter are also part of the matrix. The cineritic tuffs are fine-grained rocks composed of sericite, quartz, chlorite, disseminations of opaque minerals, and rare epidote. In places a weak foliation is defined by sericite lamellae.

Dacites are porphyritic rocks with fragmented plagioclase and quartz phenocrysts dispersed in a fine-grained quartzo–feldspathic matrix. In places, fine-grained chlorite, sericite, and opaque minerals form diffuse and irregular concentrations.

3.2. Matará Formation

The Matará Formation encompasses most of the basic and ultrabasic rocks of the metavolcano-sedimentary sequence of the Aurizona Group. The formation is composed of very fine-grained, dark-grey to dark metabasalt, schist, and amphibolite. Field relationships have not been observed between this formation and their country-rocks or between the Matará Formation and the other units of the Aurizona Group.

The metabasalts are normally schistose and composed of an actinolite- or fibrous actinolite–tremolite-rich matrix. White spots over this matrix comprise chlorite, epidote, zoisite, and rare sericite, which probably substitute for plagioclase. In places, clinozoi-

site is an important phase, occurring surrounded by opaque minerals.

Tremolite- and talc–tremolite-bearing schists show decussate texture, with tremolite crystals of up to 5 mm in the longest dimension showing interstitial aggregates composed of zoisite, talc, titanite, and chlorite. The light-colored portions of these schists comprise talc, chlorite, and remains of partially altered tremolite. In general, the titanite forms coronae around opaque minerals. Calcite, quartz, and plagioclase were only locally recognized. The clinozoisite–actinolite ± tremolite assemblage indicates low- to medium-grade metamorphic conditions for the metabasalts and basic/ultrabasic schists, consistent with the greenschist and epidote–amphibolite metamorphic facies.

Amphibolites, derived from the metamorphism of basic rocks, are subordinate rocks of the Matará Formation. They show long radial hornblende crystals with interstitial quartz, plagioclase and opaque minerals.

3.3. Serra do Jacaré volcanic unit

The Serra do Jacaré volcanic unit is composed of acid, intermediate and subordinate basic unmetamorphosed volcanic rocks. The petrographic types are dacite porphyry, andesite, basalt, tuff, and volcanic breccia that show gray color and lack mesoscopic tectonic fabric.

The dacite porphyry shows plagioclase and corroded quartz phenocrysts (Fig. 3b) set in a quartzo–feldspathic matrix. The plagioclase phenocrysts show compositional zoning and are partially altered to sericite, epidote, calcite, and chlorite. In some samples, fragmented crystals of plagioclase are the predominant phenocrysts. glomeroporphyritic texture, dissemination of biotite in the matrix, and concentrations of opaque minerals are features observed locally. Some dacite and andesite samples present lithic fragments in addition to euhedral phenocrysts of plagioclase and, subordinately, quartz. Andesite-basalts are medium-grained rocks with subhedral plagioclase and hornblende in addition to scarce anhedral quartz phenocrysts.

Lithic tuffs and breccias are composed of 0.5–1.0 mm-large, angular fragments of dacite porphyry and subordinately tuff, which are set in a chlorite- and calcite-rich quartzo–feldspathic matrix. Tuffs are composed of quartz fragments with titanite, calcite and epidote filling fractures within, and spaces between the fragments. Sericite also occurs both in these fractures and substitute for plagioclase. Opaque minerals are restricted to quartz fragments.

3.4. Rio Diamante Formation

The Rio Diamante Formation comprises flows and subordinate volcanoclastic deposits. In outcrop they are predominantly massive rocks with local flow structure and show dark-gray and greenish colors. All rocks are porphyritic (Fig. 3c) and, based on the type and content of phenocrysts, they are classified as rhyolite, dacite, and dacitic tuff.

Rhyolites and dacites contain quartz, plagioclase and subordinately microcline phenocrysts set in a biotite-bearing quartzo–feldspathic matrix. The feldspar phenocrysts are in general euhedral, whereas quartz shows embayment texture. Apatite, titanite, zircon, and opaque minerals occur as accessory phases. Millimeter-thick veinlets, composed of variable proportions of quartz, calcite, epidote, chlorite, stilpnomelane, and pyrite fill fractures in the volcanic rocks. Dissemination of pyrite is also a common feature. Both veinlets and disseminations are related to late-stage hydrothermal alteration.

Tuffs are composed of plagioclase and quartz phenocrysts and angular fragments of volcanic rocks set in a biotite-rich quartzo–feldspathic matrix. The biotite crystals occur in irregular convolute concentrations, possibly as a result of the magmatic flow. Rounded grains of quartz and quartz–sericite veinlets are also observed.

3.5. Rosilha volcanic unit

The Rosilha volcanic unit is still poorly defined in the geological map, because of the lack of good outcrops and of well-defined field relationships with other units, occurring mainly as sparse blocks in a restricted area. It is composed of tuffaceous rocks and subordinate flows and both are petrographically similar to the rocks of the Rio Diamante formation. The petrographic types are lithic tuff, crystal tuff, rhyolite, and dacite. The lithic tuffs present fragmental texture characterized by fragments of volcanic rocks and of plagioclase (70%) and quartz (30%) set in a quartzo–feldspathic matrix. Plagioclase phenocrysts show compositional zoning and are partially altered to sericite, epidote, and chlorite. Quartz phenocrysts show embayment texture and are, in places, broken.

Crystal tuffs show phenocrysts and fragments of quartz and plagioclase, and subordinate *K*-feldspar and biotite set in a quartzo–feldspathic matrix. The fragment/phenocryst ratio is variable. The phenocrysts are rarely euhedral, frequently broken and showing cusp shapes. Plagioclase shows compositional zoning and quartz is corroded. Some light-colored portions of the matrix may represent fragments of finer-grained volcanic rocks, shards and irregular flow structure with convolute folds.

Rhyolites and dacites (Fig. 3d) are gray-colored porphyritic rocks with plagioclase and anhedral quartz phenocrysts. The matrix is composed of quartz, feldspars and agglomerates of amphibole that may surround the phenocrysts. Zircon and apatite are accessory phases.

4. Geochronology

Zircon crystals from three samples of volcanic rocks of the Serra do Jacaré, Rio Diamante and Rosilha units have been dated using the U–Pb SHRIMP (Compston et al., 1984; Williams, 1998) and Pb-evaporation (Kober, 1986) methods. Analytical procedures are summarized in the Appendix A and results are given in Tables 1 and 2.

4.1. U–Pb SHRIMP results

Sample EK179 is a dacite porphyry of the Rio Diamante Formation (Fig. 3c). Zircon crystals of this sample are variable in size, shape and form, but most are anhedral and fragmented. The majority of the analyzed zircon crystals plot as a cluster on or near the concordia (Fig. 4). Nine of these combine to give a concordia age of 2159.7 ± 7.6 Ma that is interpreted as being the crystallization age of the volcanic rock. Some other analyses do not fall into this group. Zircon 9.1 is clearly an inherited grain that gives an apparent age of about 2957 Ma (Table 1 and Fig. 4). Grains 1.1 and 15.1 give lower apparent ages of 1897 and 2079 Ma. They are similar to the rest of the population and are only distinguished by Th/U ratios greater than 1.0 (Table 1). This precludes metamorphism, which is in line with the unmetamorphosed character of the volcanic rock. These ratios are also distinct from normal magmatic ratios.

It appears that the U–Th–Pb system behaved open for these crystals, and the cause of this behavior is not fully understood. The age of 2079 Ma is similar to the age of the peraluminous magmatism found in the São Luís Craton and basement of the Gurupi Belt, which has been interpreted as associated with metamorphism and crustal melting (Palheta, 2001; Klein et al., 2005b). This age is also similar to the age of 2056–2076 Ma found in a granitic unit dated by Klein et al. (2008) that has been interpreted as representing the post-orogenic magmatism in the São Luís Craton. Therefore,

Table 1
Summary of U–Pb SHRIMP zircon data from sample EK179 (dacite porphyry) of the Rio Diamante Formation

Zircon/spot	% $^{206}Pb_c$	ppm U	ppm Th	$^{232}Th/^{238}U$	ppm$^{206}Pb^*$	(1) $^{206}Pb/^{238}U$ Age (Ma)	(1) $^{207}Pb/^{206}Pb$ Age (Ma)	% Discordant	(1) $^{207}Pb^*/^{206}Pb^*$	±%	(1) $^{207}Pb^*/^{235}U$	±%	(1) $^{206}Pb^*/^{238}U$	±%
1.1	0.09	277	287	1.07	80.5	1878 ± 18	1897 ± 18	1	0.1161	1	5.411	1.3	0.3381	0.86
2.1	–	224	95	0.44	77.9	2189 ± 21	2164 ± 9.2	−1	0.135	0.53	7.528	1	0.4044	0.89
3.1	0.04	101	39	0.39	35.1	2184 ± 23	2154 ± 10	−1	0.13423	0.6	7.462	1.2	0.4032	1.1
4.1	0.03	251	109	0.45	84.4	2127 ± 20	2146.9 ± 6.8	1	0.13369	0.39	7.207	0.95	0.391	0.87
5.1	0.20	63	18	0.30	22	2199 ± 27	2163 ± 17	−2	0.1349	0.96	7.56	1.6	0.4066	1.3
6.1	1.18	1320	3822	2.99	250	1267 ± 12	2387 ± 17	47	0.1538	0.99	4.601	1.3	0.2172	0.78
7.1	0.06	1129	538	0.49	253	1496 ± 14	2126.3 ± 4.2	30	0.13212	0.24	4.757	0.81	0.2611	0.78
8.1	0.09	141	54	0.40	49.6	2211 ± 28	2179.4 ± 9.5	−1	0.1362	0.55	7.68	1.4	0.4091	1.3
9.1	0.26	36	34	0.98	18.4	3022 ± 39	2956 ± 12	−2	0.2167	0.77	17.87	1.6	0.5982	1.4
10.1	0.27	270	123	0.47	92.6	2156 ± 20	2153.8 ± 8.4	0	0.13423	0.48	7.35	0.99	0.3972	0.87
11.1	–	141	48	0.35	48.2	2160 ± 22	2158.1 ± 9.3	0	0.13454	0.53	7.383	1.1	0.398	0.97
12.1	0.29	89	28	0.32	30.4	2146 ± 23	2168 ± 14	1	0.1353	0.8	7.368	1.3	0.395	1.1
14.1	0.20	319	183	0.59	105	2082 ± 19	2172 ± 13	4	0.1356	0.75	7.131	1.1	0.3813	0.84
15.1	0.00	107	124	1.20	35.2	2098 ± 22	2079 ± 10	−1	0.12863	0.57	6.821	1.2	0.3846	1

Errors are 1σ; Pbc = common Pb; Pb* = radiogenic Pb; (1) = common Pb corrected using measured ^{204}Pb.

Table 2
Summary of single zircon Pb-evaporation results for sample EK22C (andesite) of the Serra do Jacaré volcanic unit, and sample EK16 of the Rosilha volcanic unit

Zircon	T (°C)	No. of ratios	$^{204}Pb/^{206}Pb$	2σ	$^{208}Pb/^{206}Pb$	2σ	$(^{207}Pb/^{206}Pb)^a$	2σ	Age (Ma)	2σ
Serra do Jacaré volcanic unit										
C/2	1500	16/16	0.000145	0.000013	0.06741	0.0009	0.13531	0.00087	2168.4	11.2
C/5	1500	14/14	0.000108	0.000040	0.06440	0.00692	0.13542	0.00070	2169.8	9.0
C/6	1450	4/4	0.000238	0.000022	0.05614	0.00125	0.13483	0.00031	2162.3	4.0
C/8	1500	32/32	0.000242	0.000014	0.05846	0.00119	0.13483	0.00054	2162.2	7.0
		66/88					Mean age		2163.6	3.2
Rosilha volcanic unit										
16A/1	1500	20/34	0.000358	0.000013	0.27207	0.00141	0.11759	0.00062	1920	10
16B/2	1500	30/30	0.000075	0.000004	0.20277	0.00134	0.11990	0.00034	1955	5
16 A/6	1500	6/6	0.000282	0.000034	0.23100	0.00196	0.12030	0.00101	1961	15
16 A/4	1500	38/38	0.000105	0.000004	0.24772	0.00105	0.12396	0.00023	2014	3
16 A/3	1450	8/8	0.000000	0	0.15245	0.00129	0.12537	0.00123	2034	17
16 A/7	1500	32/32	0.000247	0.000011	0.12777	0.00078	0.12539	0.00046	2035	6
16 A/5	1500	32/32	0.000090	0.000025	0.18307	0.00090	0.12781	0.00054	2068	7
16C/7	1450	32/32	0.000132	0.000008	0.11021	0.00061	0.13433	0.00018	2156	2
16C/3	1500	24/24	0.000035	0.000012	0.10954	0.00094	0.13500	0.00098	2165	13

[a] Corrected according to Stacey and Kramers (1975).
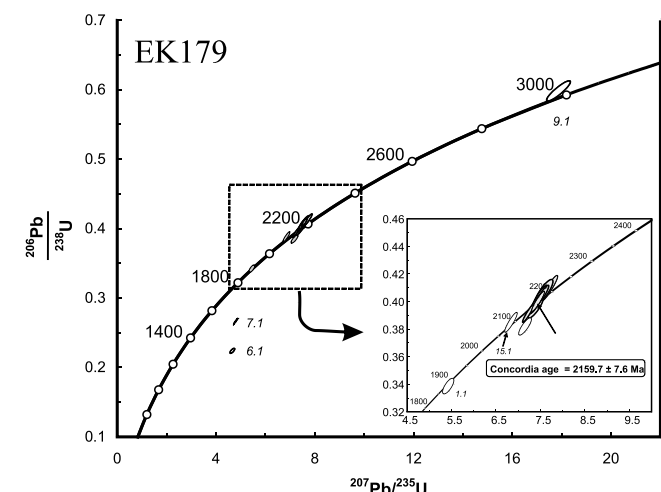
Fig. 4. SHRIMP U–Pb zircon concordia plots for a dacite porphyry sample of the Rio Diamante Formation.

fluids from one of these magmatic events could have caused lead loss associated with (partial) resorption and reprecipitation of the zircon crystal. The younger zircon crystal might have also been affected by this mechanism, although an event with this age is unknown in the region so far. A very similar and enigmatic situation has been described by Poujol et al. (2005) for an undeformed volcanic sequence of the Kaapvaal Craton of Southern Africa.

4.2. Pb-evaporation results

Sample EK22C is an andesite of the Serra do Jacaré volcanic unit. The analyzed zircon crystals are mostly fragmented portions of relatively large (0.3–0.6 mm) subhedral grains. Some are fractured, but clear and in general devoid of solid inclusions. Four crystals gave ages between 2162 ± 7 Ma and 2170 ± 9 Ma that overlap within analytical uncertainties. These crystals yielded a mean age of 2163.6 ± 3.2 Ma (Table 2), which is interpreted as the crystallization age of the volcanic rock.

Sample EK16 is a dacite of the Rosilha volcanic unit (Fig. 3d). Zircon grains are very small (<0.3 mm). Some crystals are elongated, euhedral to subhedral; other crystals are short and subhedral to rounded in shape. Nine crystals gave very distinct ages between 1920 ± 10 Ma and 2165 ± 13 Ma that are broadly distributed in three different age patterns: 1920–1962 Ma; 2014–2068 Ma; 2156–2165 Ma (Table 2). The lower ages are more probably related to the opening of the isotopic system with Pb loss after the crystallization. Two alternatives are envisaged to explain the other two age intervals: (1) the oldest interval reflects the crystallization age of the volcanic rock and the younger is also related to Pb loss; (2) the younger interval is considered the crystallization age of the volcanic rock and the oldest represents inheritance. Most of the igneous rocks of the São Luís Craton formed at about 2150–

Table 3
Whole-rock Sm–Nd data

Sample	Rock type	Age (Ma)	Sm (Ma)	Nd (ppm)	$^{147}Sm/^{147}Nd$	$^{143}Nd/^{144}Nd$	2σ (10^{-6})	$\varepsilon Nd(0)$	$\varepsilon Nd(t)$	T_{dm}
Pirocaua Formation (Aurizona Group)										
PF1A	Metadacite	2240[b]	1.94	8.62	0.1363	0.511789	12	−16.6	+0.8	2.48[a]
Serra do Jacaré volcanic unit										
EK22C	Dacite	2164	2.49	12.55	0.1202	0.511597	18	−20.3	+ 1.0	2.37
AF534	Andesite	2164	4.60	21.82	0.1276	0.511703	19	−18.2	+ 1.0	2.38
Rio Diamante Formation										
EK159	Rhyolite	2159	7.21	32.69	0.1333	0.511831	7	−15.7	+ 1.8	2.31
EK179	Dacite	2159	7.76	35.17	0.1334	0.511802	16	−16.3	+ 1.2	2.37
EK183	Tuff	2159	7.15	32.56	0.1328	0.511821	13	−15.9	+ 1.7	2.31
Rosilha volcanic unit										
EK12* 2160	Dacite	2068[b]	2.80	14.92	0.1133	0.511457	4	−23.0	−0.9	2.42[1]
EK16A	Rhyodacite	2068[b] 2160[b]	6.72	30.12	0.1349	0.511761	20	−17.1	−0.7 +0.04	2.50

Key for references: data from this study, unless where references are quoted.
[a] Klein et al. (2005a).
[b] Assumed age.

2160 Ma, which favors the first explanation, and the same reasoning discussed above for the SHRIMP analysis of the Rio Diamante formation sample may apply in this case. However, a younger volcanic event occurring at about 2068 Ma cannot be ruled out, since similar ages are found in peraluminous granites in both the São Luís Craton and Gurupi Belt and because of differences in the geochemical and Nd isotope behavior (see below) presented by the Rio Diamante and Rosilha units. We do not have any elements to decide between these two hypotheses. Only geochronological techniques using better spatial resolution (SHRIMP, LA–ICP–MS) could help in the solution of this problem.

5. Nd isotopes

Sm–Nd isotope compositions were determined in whole rock samples from the Serra do Jacaré, Rio Diamante, and Rosilha units. Analytical procedures (Gioia and Pimentel, 2000) are described in the Appendix A. The results are presented in Table 3 along with previous results (Klein et al., 2005a) for the Pirocaua and Rosilha units. Two groups of data can be observed, with T_{DM} model ages of 2.31–2.38 Ga occurring in the Serra do Jacaré and Rio Diamante units, and 2.42–2.50 Ga, detected in the Pirocaua and Rosilha units. The two samples of the Serra do Jacaré unit have nearly the same values of T_{DM} of 2.37 and 2.38 Ga, both with $\varepsilon Nd(t)$ value of +1.0. The three samples of the Rio Diamante Formation have model ages between 2.31 and 2.37 Ga, with $\varepsilon Nd(t)$ values ranging from +1.2 to +1.8 (Table 3). A metadacite of the Pirocaua Formation yielded a T_{DM} model age of 2.48 Ga, with $\varepsilon Nd(t)$ value of +0.8. Two samples of the Rosilha unit show model ages of 2.42 and 2.50 Ga. The $\varepsilon Nd(t)$ value is dependent on the crystallization age of the sample. Considering that the age of the Rosilha unit could not be established, the $\varepsilon Nd(t)$ value was calculated for 2068 Ma and 2165 Ma (the two possibilities discussed in the previous section). Accordingly, $\varepsilon Nd(t)$ values between −0.9 and +0.1 have been obtained, respectively, for each possible age (Table 3).

6. Geochemistry and petrogenetic aspects

Whole rock geochemical results for the metavolcanic and volcanic rocks are presented in Tables 4–6. When submitted to hydrothermal alteration and/or metamorphism volcanic rocks show considerable mobility of major elements, especially the alkalis, and of trace-elements such as Rb, Sr, and Ba. Therefore, geochemical classification of volcanic rocks based on these elements must be taken with caution. Other elements, such as V, Ti, Zr, Y, Nb, Ga, Sc, and REE are thought to be relatively immobile under alteration/metamorphic conditions (Watters and Pearce, 1987; Rollinson, 1993). In fact, analyzed samples from three of the studied units (Matará, Pirocaua and Serra do Jacaré) show moderate to high LOI values (Tables 4 and 5), indicating alteration. As such, in this study the geochemical characterization of the volcanic rocks is mainly based on immobile elements, and the chemical classification is that of the Nb/Y versus Zr/TiO₂ discrimination diagram of Winchester and Floyd (1977) (Fig. 5). Accordingly, the samples of the Matará Formation plot in the limits of the subalkaline basalt and andesite fields with the field of andesite/basalt rocks; those of the Pirocaua Formation plot in the limit of the andesite field with the fields of andesite/basalt and rhyodacite/dacite; the Serra do Jacaré Formation is composed mostly of andesite and subordinately of andesite/basalt and subalkaline basalt; and both the Rosilha and Rio Diamante units plot within the field of rhyodacite/dacite (Fig. 5).

6.1. Matará Formation

In the MORB-normalized multi-element diagram (Fig. 6a) sample EK87 (talc–tremolite schist) shows contents and distribution that are typical of ocean island arc tholeiites, whereas the pattern of sample EK101A (tremolite schist) resembles that of the ocean island arc high-K calc-alkaline basalts (e.g., Watters and Pearce, 1987; Wilson, 1989), despite the pronounced Ce and Sm anomalies. Sample EK89 (amphibolite) does not show any characteristic pattern, which, despite the low LOI value, is probably due to LILE mobility during metamorphism and deformation.

The REE contents vary from 17 to 410 ppm in distinct samples. Nevertheless, samples of talc–tremolite schist and amphibolite from the same area show similar flat patterns (Fig. 6b) with La/Yb(n) = 1.0–1.4 (Table 4). These patterns have similarities with those of tholeiitic basalts from both marginal (back-arc) basins (e.g., Wilson, 1989) and Paleoproterozoic Birrimian basalts that have been interpreted to have formed in island arcs (Sylvester and Attoh, 1992). The flat distribution implies shallow MORB-type mantle in magma generation (Winter, 2001).

The negative Ce anomaly (Fig. 6b) presented by two samples indicates association with oceanic environment, since the sea water is depleted in Ce (Day et al., 2000). This anomaly may be produced by at least three different mechanisms: (1) intense alteration of basic lavas deposited on the sea floor caused by interaction with the sea water (Ludden and Thompson, 1979); (2) presence of subducted marine sediments in the genesis of island arc basic magmas (Hole et al., 1984; Shimizu et al., 1992);

Table 4
Whole rock chemical data for metavolcanic rocks of the Matará and Pirocaua formations (Aurizona Group)

	Matara Formation			Pirocaua Formation	
	EK101A tremolite-schist	EK87 talc-tremolite-schist	EK89 amphibolite	EK168A dacite	EK60B andesite basalt
SiO_2 (wt%)	45.74	48.33	58.01	71.22	78.93
Al_2O_3	12.33	14.67	10.52	13.51	7.93
Fe_2O_3	12.26	9.33	19.69	5.49	4.2
MgO	20.15	11.66	0.47	0.68	2.59
CaO	7.93	14.05	6.86	0.19	0.04
Na_2O	0.44	0.96	1.71	3.43	0.15
K_2O	0.04	0.16	0.32	2.23	1.17
TiO_2	0.38	0.46	1.57	0.67	0.34
P_2O_5	0.03	0.06	0.58	0.14	0.05
MnO	0.21	0.14	0.26	0.06	0.02
Cr_2O_3	0.47	0.16	0.00	0.004	0.048
LOI	6.10	2.50	0.90	2.20	4.50
SUM	99.93	99.98	99.91	99.83	99.97
Ba (ppm)	32.6	40.6	83	909	132
Co	89.8	79.8	22.2	35.7	39.2
Cs	<.l	0.3	<.l	0.9	0.9
Ga	9.9	11.3	23.4	22.5	9.2
Hf	0.6	0.8	6.7	7	1
Nb	0.7	1.2	10.1	8.2	1.5
Rb	1.3	3	2.8	60.3	37.6
Sn	bd	bd	1	2	bdl
Sr	25	152	111	113	46
Ta	<.l	<.l	0.7	0.6	0.1
Th	<.l	0.1	0.9	4.1	0.9
U	<.l	<.l	0.2	1.6	2.4
Sc	32	37	**33**	15	17
V	177	165	bd	13	107
W	25	125	65	151	3
Zr	20	23	208	231	41
Y	97	9	242	52	18
Mo	0.2	0.6	0.7	0.5	1.3
Cu	142	270	8	113.8	90
Pb	2.2	0.4	0.8	9.7	2.6
Zn	47	16	104	75	60
Ni	603	167	6	15.5	96.7
La	82.6	1.6	34.1	28.9	8.1
Ce	9.1	4.5	70.9	64.9	17.6
Pr	34.9	0.67	13.43	8.4	2.45
Nd	139.5	2.8	66.5	35.9	12.8
Sm	33.1	1.3	23.7	8.5	2.4
Eu	12.78	0.49	7.75	2.4	0.73
Gd	25.58	1.43	29.68	7.69	2.7
Tb	5.23	0.28	5.79	1.4	0.42
Dy	31.44	1.5	33.42	8.16	2.78
Ho	5.17	0.37	7.69	1.8	0.51
Er	13.72	1.11	21.91	5.41	1.47
Tm	1.92	0.18	3.03	0.82	0.27
Yb	13.44	1.03	18.52	5.29	1.39
Lu	1.76	0.15	2.77	0.82	0.24
ΣREE	410.24	17.41	339.19	180.4	53.9
Eu/Eu^*	1.3	1.1	0.9	0.9	0.9
LaN/YbN	4.1	1.0	1.2	3.7	3.9
LaN/SmN	1.6	0.8	0.9	2.1	2.1
CeN/YbN	2.7	1.4	1.2	1.3	1.5
CeN/SmN	0.2	1.1	1.0	3.2	3.3
EuN/YbN	0.1	0.8	0.7	1.8	1.8

bd: below detection limit.

(3) dehydration and metassomatism of the oceanic plate (Shimizu et al., 1992). Similar Ce anomalies have been reported for coeval basic rocks in the West African Craton (Abouchami et al., 1990; Sylvester and Attoh, 1992) and in the Guyana shield (Vanderhaeghe et al., 1998).

6.2. Pirocaua Formation

The two analyzed samples of the Pirocaua Formation show some similarities but also differences in their chemical composition (Table 4). In the primitive mantle-normalized spidergram (Fig. 7a) the samples show moderate fractionation between the LILE and HSFE, positive Pb and Zr anomalies, and strong negative brakes in the Nb, Ti, Sr and P elements. The samples also show distinct REE concentrations (54–180 ppm), but with sub-parallel patterns (Fig. 7b). This suggests REE fractionation in relatively constant proportions, but under variable compositional conditions, which is supported by the whole geochemical data (Table 4). These patterns are characterized by moderate fractionation between light and heavy REE (La/Yb(n) = 3.7–3.9) and absence of Eu anomaly (Table 4), which is typical of calc-alkaline suites.

Table 5
Whole rock chemical data for volcanic rocks of the Serra do Jacaré volcanic unit

	EK22B	EK185A	AF534	EK185B	EK22C
	Basalt	Andesitic basalt	Andesite	Andesite	Andesite
SiO_2 (wt%)	51.56	53.39	58.98	66.69	66.73
Al_2O_3	17.98	16.6	16.16	16.04	15.71
Fe_2O_3	12.30	10.04	8.11	4.22	4.6
MgO	4.74	3.96	2.66	1.38	1.54
CaO	7.80	7.5	4.99	2.26	4.49
Na_2O	3.39	3.17	3.63	3.32	4.23
K_2O	0.80	0.82	1.05	0.78	0.34
TiO_2	1.05	1.1	0.79	0.5	0.41
P_2O_5	0.16	0.31	0.23	0.1	0.13
MnO	0.22	0.14	0.11	0.09	0.06
Cr_2O_3	0.00	0.003	0.006	0.007	0.004
LOI	2.10	2.80	3.20	4.60	1.70
SUM	99.76	99.84	99.92	99.98	99.94
Ba (ppm)	433	393	462	376	303
Co	52.2	49.8	30.5	27.5	106.5
Cs	0.6	1	1.2	0.5	0.7
Ga	19.6	21.4	17.8	19	18.9
Hf	1.2	3.3	3.8	3	2.6
Nb	4.1	4.1	4.1	3.3	2.8
Rb	17	23.4	27.5	15.7	10
Sn	1	bd	bd	<1	2
Sr	480	545	376	440	513
Ta	0.3	0.3	0.3	0.2	0.2
Th	0.2	1.4	2.5	1.4	1.4
U	0.4	0.9	0.9	0.8	0.6
Sc	34	23	17	10	8
V	276	234	118	83	66
W	118	128	87	123	597
Zr	23	117	119	104	84
Y	26	32	24	6	8
Mo	0.6	1.4	1.1	0.4	2.4
Cu	96.9	184.6	49	16.1	46
Pb	1.1	0.8	5.8	3.5	3.3
Zn	86	106	64	43	52
Ni	5.6	14.7	13	18.4	15.4
La	13.2	18.7	18.2	9.3	9.8
Ce	34.3	41.8	39.8	18.6	23.6
Pr	5.15	5.84	5.31	1.97	3.02
Nd	25.6	28	20.8	7	13
Sm	5.2	6	4.2	1.5	2.4
Eu	1.69	1.76	1.5	0.49	0.59
Gd	4.5	5.7	4.44	1.22	1.7
Tb	0.77	0.91	0.82	0.18	0.3
Dy	4.12	6.14	3.94	1.22	1.45
Ho	0.84	1.23	0.89	0.22	0.26
Er	2.7	3.38	2.48	0.63	0.94
Tm	0.42	0.45	0.36	0.1	0.14
Yb	2.64	2.98	2.07	0.71	0.8
Lu	0.38	0.52	0.3	0.11	0.08
ΣREE	101.5	123.4	105.1	43.3	58.1
Eu/Eu*	1.1	0.9	1.1	1.1	0.9
LaN/YbN	3.4	4.2	5.9	8.8	8.3
LaN/SmN	1.6	2.0	2.7	3.9	2.6
CeN/YbN	1.8	1.7	2.1	2.0	2.1
CeN/SmN	3.4	3.6	5.0	6.8	7.6
EuN/YbN	1.6	1.7	2.3	3.0	2.4

bd: below detection limit.

6.3. Serra do Jacaré volcanic unit

The Serra do Jacaré volcanic unit presents variable SiO_2 contents of 51.5–66.7% (Table 5), consisting of a sequence with acid, intermediate and basic rocks. The La shows broadly a positive correlation with Zr and Nb, and a correlation is also observed between Zr and Nb (Fig. 8). The Zr/Nb and Nb/La ratios are relatively constant, whereas the Zr/La and Ce/Yb(n) ratios are more variable (Fig. 8). It also noticeable that La, Zr and Nb distributions form distinct domains when compared with those presented by the Rosilha and Rio Diamante rocks (Fig. 8). The three units also plot in different domains in the $\varepsilon Nd(t)$ versus Mg# diagram (Fig. 9).
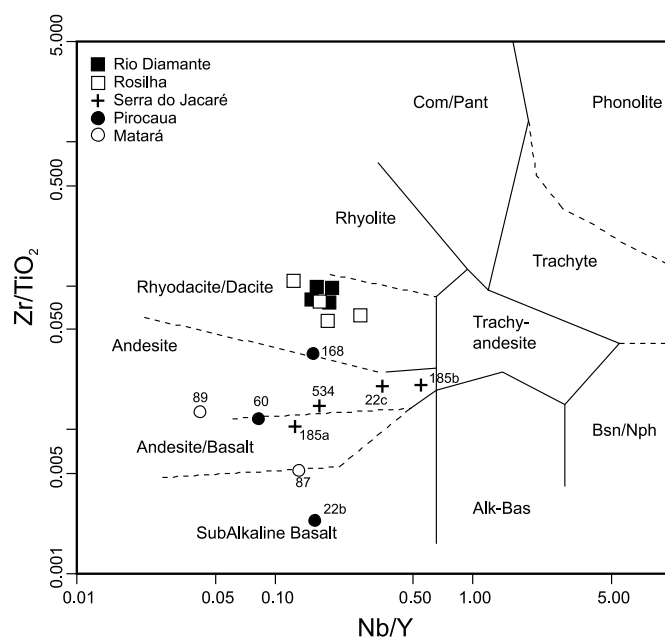
Fig. 5. Nb/Y versus Zr/TiO_2 diagram of Winchester and Floyd (1977) for the classification of volcanic rocks.

There are some differences in both concentration and distribution patterns of REE, LILE and HFSE when compared with the SiO_2 contents (Fig. 10 and Table 5). As a common feature, all samples show absence of Eu anomaly and enrichment in LILE in relation to the HFSE. Samples having 55–70 wt.% SiO_2 show REE concentrations of 43–105 ppm and have the highest fractionation between light and heavy REE (La/Yb(n) = 5.9–8.8). Samples with SiO_2 lower than 55% show less variation in the REE contents (101–123 ppm) and are only moderately fractionated (La/Yb(n) = 3.4–4.2). As a whole, silica-rich samples have normal and high-K calc-alkaline patterns, whereas the low-silica samples (EK22B and EK185A) have tholeiitic affinity.

In the primitive mantle-normalized multi-element diagram (Figs. 10a and 10d) the patterns also show differences related to the SiO_2 contents. Accordingly, the silica-depleted rocks are more enriched in trace elements when compared with the primitive mantle values. As a whole, the negative Nb and Ti anomalies increase, and the La and Ce contents decrease with increasing SiO_2 contents. Pb, which in the low-silica rocks forms weak negative breaks, displays prominent positive anomalies in the silica-rich terms.

6.4. Rio Diamante Formation

The Rio Diamante flows and tuffs present little chemical variation (Table 6). All samples are acidic (SiO_2 72–74 wt.%), medium-K calc-alkaline rocks. They are metaluminous, but plot near the boundary between the metaluminous and peraluminous fields (Fig. 11), which is consistent with the presence of biotite in the microcrystalline matrix.

The REE have total contents between 169 and 187 ppm and their distribution reflects little fractionation between light and heavy REE (La/Yb(n) = 3.5–3.8). This weak fractionation is essentially produced by the light REE, since the heavy REE display a rather flat pattern (Fig. 12a). Weak Eu anomalies are given by Eu/Eu* ratios of 0.6–0.8 (Table 6), which is in keeping with the moderately evolved calc-alkaline character of these rocks.

The primitive mantle-normalized multi-element diagram (Fig. 12b) shows positive Pb and pronounced negative P and Ti
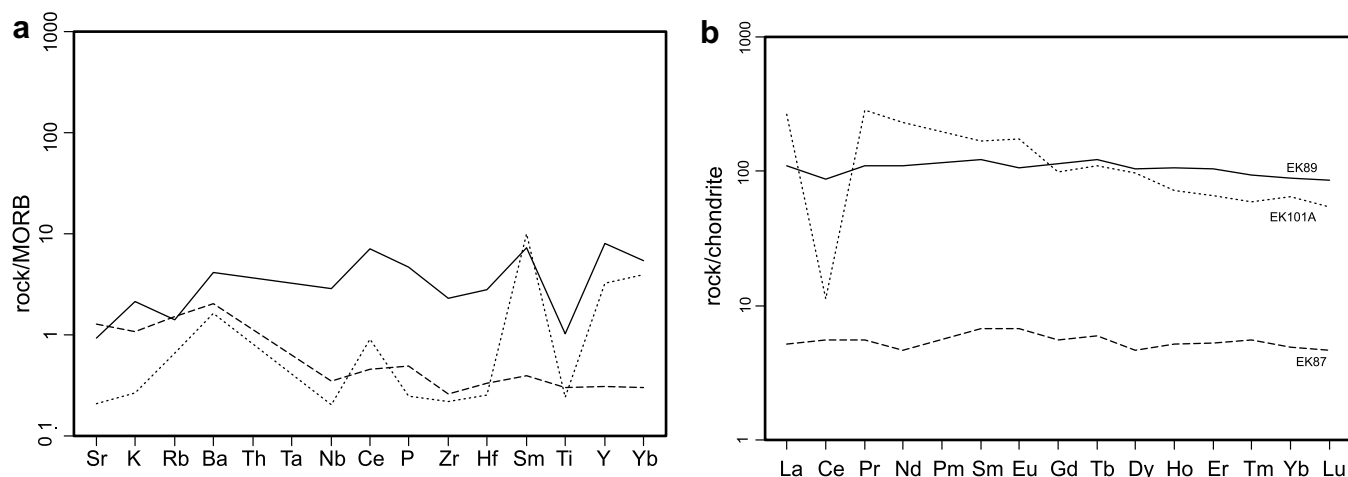
Fig. 6. (a) trace element spidergram and (b) REE plot (normalized according to Boynton, 1984) for the metavolcanic rocks of the Matará Formation.
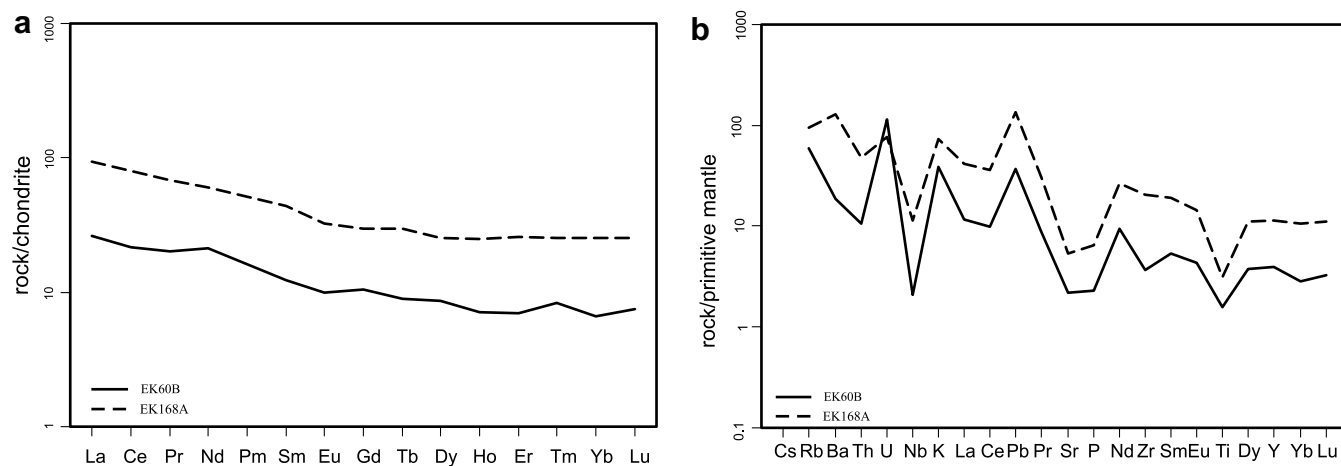

Fig. 7. (a) trace element spidergram and (b) REE plot (normalized according to Boynton, 1984) for the metavolcanic rocks of the Pirocaua Formation.

anomalies, in addition to enrichments in LILE, U, and Th in relation to the REE and HFSE.

6.5. Rosilha volcanic unit

The volcanic and tuffaceous rocks of the Rosilha unit are chemically similar to the rocks of the Rio Diamante Formation, although the Rosilha rocks show more variability. The rocks are also acidic (SiO_2 68–77 wt.%), with medium-K calc-alkaline and weakly peraluminous character (Fig. 11). The Rosilha rocks present slightly lower Ba, Hf, Nb, Zr and Y, and higher Sr and Th concentrations (or averages) when compared to the Rio Diamante rocks (Table 6). The Zr/La, Zr/Nb e Ce/Yb(n) ratios are similar in the two units, but also more variable in the Rosilha unit (Fig. 8).

The REE contents range from 136 to 177 ppm and the fractionation between light to heavy elements is slightly more pronounced in the Rosilha rocks that have La/Yb(n) ratios of 3.0–12.2 (Table 6). The heavy REE pattern is relatively flat (Fig. 13a) but with very variable chondritic enrichments, given by Ce/Yb(n) ratios of 0.5–1.1. The negative Eu anomaly is more pronounced in the Rosilha (Eu/Eu* = 0.4–0.7) than in the Rio Diamante rocks (Table 6 and Figs. 12a and 13a). The trace element distribution is also very similar to that of the Rio Diamante Formation, but the Rosilha rocks display a sharp negative break in the Nb enrichment (Figs. 12b and 13b).

7. Discussion: tectonic setting and crustal evolution

Klein et al. (2005a) based on zircon geochronology and Nd isotope data, mostly on granitoids, interpreted the Paleoproterozoic evolution of the São Luís Craton, in its present-day configuration, as occurring in at least three (not necessarily unique) periods: ~2240 Ma, 2168–2147 Ma, and 2100–2090 Ma. Those authors have also shown that the Paleoproterozoic rocks derived mostly from juvenile protoliths and only subordinate relics of a remobilized Archean crust have been indicated by Nd isotopes studies of S-type granites. Furthermore, the association of volcano-sedimentary rocks with large masses of juvenile calc-alkaline granitoids has been interpreted as reflecting an intra-oceanic, arc-related subduction setting for this association.

According to Klein et al. (2005a) the orogenic evolution of the São Luís Craton started sometime before 2240–2260 Ma (age of a metapyroclastic rock of the Pirocaua Formation), with the opening of an ocean basin approximately at the Archean–Paleoproterozoic boundary. The model ages of 2.48–2.42 Ga found in metadacite and dacite (in this paper characterized as belonging to the Pirocaua Formation and Rosilha volcanic unit, respectively) have been interpreted as recording the age of the mafic protoliths (oceanic crust) that formed at that time and that were subsequently melted. After that, large masses of calc-alkaline granitoids of the Tromaí Intrusive Suite were produced between 2168 and 2147 Ma and related
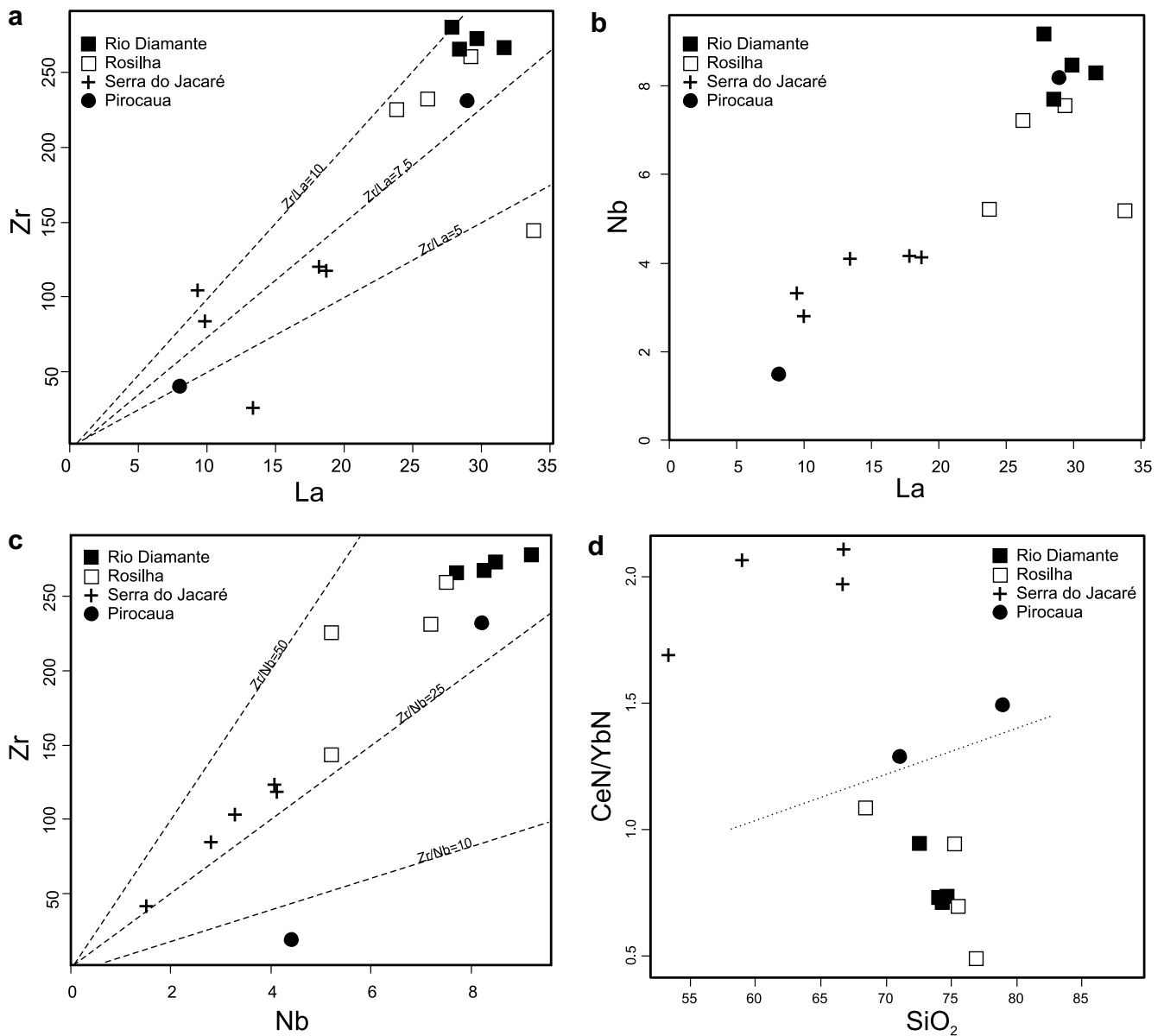
Fig. 8. Trace element relationships of volcanic and metavolcanic rocks of the São Luís Craton.

to mantle wedge and/or oceanic plate subduction. This period has been considered to represent the accretionary phase of the Paleoproterozoic orogeny. The collision phase has been related to the intrusion of muscovite-bearing granitoids (Tracuateua Suite, Fig. 1) at about 2100 Ma that were produced by melting of pre-existing continental crustal. This phase is better represented in the basement of the Gurupi Belt (Klein et al., 2005b) (Fig. 1).

This interpretation is sustained here in its broader aspects, and despite the reconnaissance character of the geochemical study presented in this paper, some interpretations can be drawn from the integrated field, petrographic, geochemical, and isotopic data, regarding the magmatic evolution and the tectonic setting in which formed the different volcanic and metavolcanic sequences of the São Luís Craton. Accordingly, volcanic pulses have been recognized in at least two, possibly three, periods of the Rhyacian evolution.

7.1. Early volcanic stage

The first volcanic stage took place at 2240 Ma and is represented by the Pirocaua and Matará formations of the metavolcano-

sedimentary Aurizona Group. The Pirocaua Formation holds calc-alkaline volcanic rocks whereas the Matará Formation is composed of tholeiites and high-K calc-alkaline basalts. Limited Nd isotope information suggests that these rocks may have formed from protoliths that had experienced short crustal residence time in addition to minor Archean component. These metavolcanic rocks are here interpreted as belonging to a volcanic arc system that might include some back-arc components. It is uncertain if this metavolcano-sedimentary succession represents remains of a distinct first arc or an early phase of a long-lived arc system.

7.2. Main arc stage

The period between about 2168 and 2150 Ma corresponds to the main constructional phase of an arc system in which developed most of the rocks of the present-day São Luís Craton. This phase is chiefly comprised of voluminous batholiths of the juvenile calc-alkaline granitoids of the Tromaí Intrusive Suite (Klein et al., 2005a) that represent deep to intermediate portions of an arc setting. Again, this may represent a second arc that accreted into
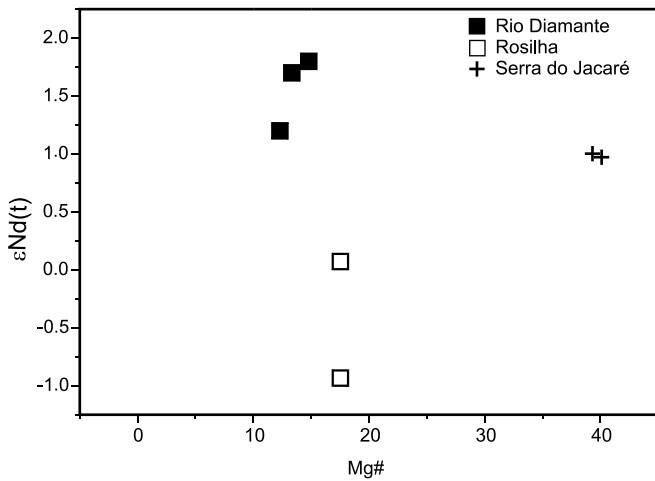
Fig. 9. Mg# versus $\varepsilon Nd(t)$ diagram showing that samples of different volcanic sequences plot in distinct domains of the diagram.

a precursor arc (Aurizona Group) or a stage of a protracted arc system.

Volcanism has also been associated to this phase and most of these volcanic rocks have probably been eroded away, since they represented the shallow portions of the arc system. The andesites, basaltic andesites and basalts of the Serra do Jacaré volcanic unit (2164 ± 3 Ma) are likely preserved products of this phase, although

the definition of the tectonic setting of this unit, if mature arc or active continental margin, is not straightforward.

The chemical composition of the of the felsic and intermediate volcanic rocks of the Serra do Jacaré unit is consistent with normal to high-*K* calc-alkaline suite. Some trace element relationships, such as Rb versus Y + Nb, Th/Yb versus Ta/Yb, and Sc/Ni versus La/Yb indicate either volcanic arc or active continental margin settings for the andesitic rocks (Fig. 14). On the other hand, the low (<1.5) and relatively constant Fe/Mg ratios, and the low (1.5–2.1) Ce/Yb ratios (Fig. 8D) are more compatible with an arc setting. The Nd isotope data indicate that the felsic to intermediate volcanism involved juvenile materials in addition to older Paleoproterozoic crustal sources. These sources may be erosive products of the early volcanic arc stage, probably without Archean contribution. The isotopic data maybe explains the geochemical pattern. The sample of basalt (EK22B) shows complex chemical relationships that tend variably to island arc, MORB and intra-plate basalts (Fig. 15). This complex geochemistry is, however, commonly shown by basalts of back-arc basins, since the genesis of this type of magmas involve mantle components modified by subduction and by magmas produced in oceanic spreading centers (Wilson, 1989). In fact, a back-arc setting is suggested by the La–Nb–Y and V–Ti relationships (Fig. 15) and the Y concentration (Table 5).

7.3. Continental margin stage

The whole rock geochemistry of the calc-alkaline volcanic and tuffaceous rocks of the Rio Diamante and Rosilha units indicates
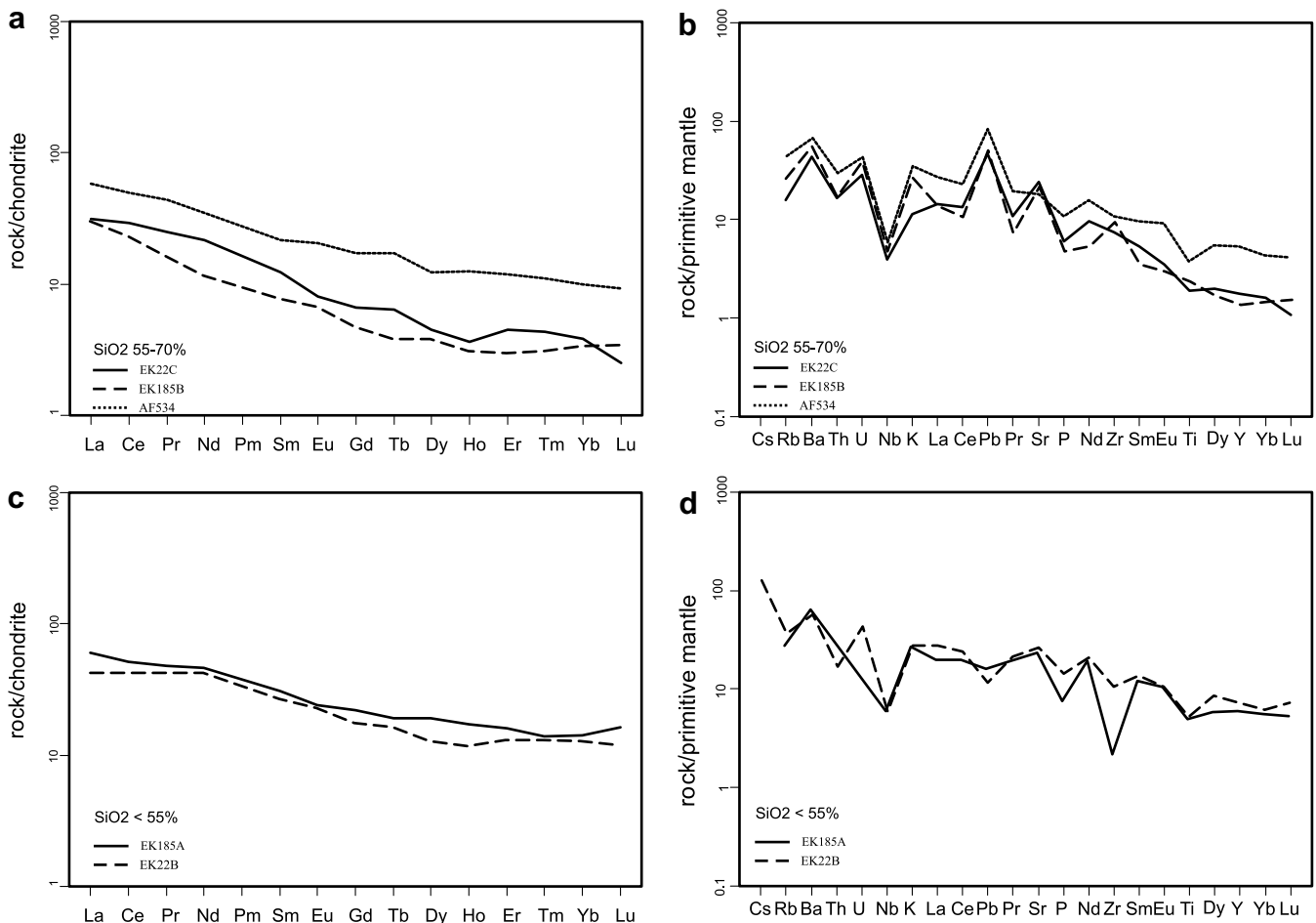

Fig. 10. Trace element and REE (normalized according to Boynton, 1984) plots for volcanic rocks of the Serra do Jacaré volcanic unit.

Table 6
Whole rock chemical data for volcanic rocks of the Rio Diamante Formation and Rosilha volcanic unit

	Rio Diamante Formation				Rosilha volcanic unit			
	EK179	EK183	EK155	EK159	AF331A	AF333A	AF335	EK16A
	Dacite	Dacite	Dacite	Dacite	Dacite	Dacite	Dacite	Dacite
SiO_2 (wt%)	72.62	74.02	74.42	74.72	68.45	75.23	75.33	77.05
Al_2O_3	12.44	12.67	12.24	12.31	14.88	13.42	12.71	10.4
Fe_2O_3	3.53	3.09	3.13	3.08	4.21	1.86	1.59	3.82
MgO	0.25	0.24	0.26	0.27	1.05	0.38	0.13	0.41
CaO	1.41	1.08	1.29	1.39	2.97	1.17	0.62	1.5
Na_2O	4.01	4.3	4.09	4.39	3.63	3.08	3.94	2.81
K_2O	3.76	3.25	3.15	2.5	2.3	3.18	3.57	1.58
TiO_2	0.32	0.32	0.28	0.29	0.38	0.22	0.33	0.21
P_2O_5	0.05	0.05	0.04	0.04	0.09	0.05	0.03	0.04
MnO	0.08	0.07	0.06	0.07	0.07	0.04	0.05	0.1
Cr_2O_3	0.002	0.002	0.001	0.002	0.003	0.001	0.001	0.001
LOI	1.3	0.7	0.9	0.8	1.8	1.2	1.4	2.0
SUM	99.77	99.79	99.86	99.87	99.84	99.84	99.71	99.92
Ba (ppm)	1167	1266	995	919	1017	1257	1006	598
Be	2	2	2	1	bdl	1	1	1
Co	29.2	46.9	30.4	36.3	37.5	40.5	35.2	34.9
Cs	1.2	2.1	0.5	1.8	1.6	2.1	0.7	1.3
Ga	19	17.8	15.8	16.9	17.4	14.4	16.2	11.5
Hf	8	7.8	7.4	7.8	7	4.9	9	7.3
Nb	8.3	7.7	8.5	9.2	5.2	5.2	7.5	7.2
Rb	70.5	82.2	62.5	62.5	62.3	94.8	68.5	41.5
Sn	2	2	2	2	1	1	2	2
Sr	185	155	157	155	354	250	100	119
Ta	0.7	0.6	0.5	0.6	0.5	0.5	0.7	0.5
Th	3.6	4.3	3.9	3.8	4.1	9	4.6	3.4
U	1.6	1.7	1.9	1.7	1.6	3.5	1.6	1.5
Sc	7	7	6	7	10	3	6	6
V	bd	bd	bd	bd	40	11	bd	bd
W	224	335	229	253	222	278	249	242
Zr	267	266	273	280	225	143	260	232
Y	54	44	51	51	28	19	44	57
Mo	1.9	5.4	2.8	2.2	1	1.6	1	0.6
Cu	85.4	121.8	42.3	26.1	32.4	6.3	7.5	15.1
Pb	19.6	2.9	4.3	3.6	4.7	10	10.3	11.5
Zn	160	52	60	68	72	39	61	72
Ni	2.1	3.6	3.1	3.7	4.7	5.3	3.4	2.7
La	31.7	28.6	29.8	27.9	23.9	33.9	29.2	26.1
Ce	66.4	64.1	64.2	63.4	53.4	67	67.9	56.3
Pr	9.04	8.36	7.91	7.86	6.35	7.05	8.39	7.39
Nd	38.3	34.2	34	31.9	28.4	25.6	35.3	28.5
Sm	8.1	7.7	7.1	7.5	5.7	4.7	8.3	6
Eu	1.92	1.41	1.33	1.34	1.18	0.62	1.1	1
Gd	7.44	6.58	6.51	7.21	4.75	2.98	6.85	6.84
Tb	1.28	1.26	1.3	1.28	0.89	0.58	1.36	1.31
Dy	8.89	7.51	6.58	7.8	4.13	3.05	7.14	7.59
Ho	1.88	1.67	1.62	1.61	0.95	0.59	1.45	1.76
Er	5.35	4.83	4.93	4.87	3.17	1.78	4.55	6.52
Tm	0.81	0.82	0.77	0.75	0.37	0.29	0.71	0.89
Yb	5.8	5.47	5.29	5.28	3.11	1.88	4.47	5.93
Lu	0.88	0.83	0.73	0.84	0.41	0.25	0.72	0.8
ΣREE	187.8	173.3	172.1	169.5	136.7	150.3	177.4	156.9
Eu/Eu_*	0.8	0.6	0.6	0.6	0.7	0.5	0.4	0.5
La_N/Yb_N	3.7	3.5	3.8	3.6	5.2	12.2	4.4	3.0
La_N/Sm_N	2.5	2.3	2.6	2.3	2.6	4.5	2.2	2.7
Ce_N/Yb_N	0.9	0.7	0.7	0.7	1.1	0.9	0.7	0.5
Ce_N/Sm_N	3.0	3.0	3.1	3.1	4.4	9.2	3.9	2.5
Eu_N/Yb_N	2.0	2.0	2.2	2.0	2.3	3.4	2.0	2.3

bd: below detection limit.

that these rocks may have formed through at least two mechanisms: (1) partial melting of mantle material followed by fractional crystallization; (2) melting of calc-alkaline rocks, i.e., reworking of island arc materials (Tromaí Intrusive Suite, Aurizona Group). The presence of inherited zircon of Archean age in the Rio Diamante Formation, and the Nd isotope data indicating that the rocks of the Rio Diamante Formation formed from juvenile protoliths and/ or from materials that experienced short crustal residence time, with very limited participation of Archean materials, favors the second of the proposed mechanisms or a combination of the two.

Furthermore, even if one assumes that the Rio Diamante and Rosilha units are coeval, and despite the petrographic and some geochemical similarities between these two units, other geochemical aspects and the Nd isotopes results indicate that they crystallized from distinct magma sources and/or they underwent different magmatic evolution.

As a whole, the geochemical and isotopic information, in addition to the unmetamorphosed and undeformed character of the Rio Diamante volcanic rocks hints an orogenic character with emplacement in an active continental margin or in a transitional
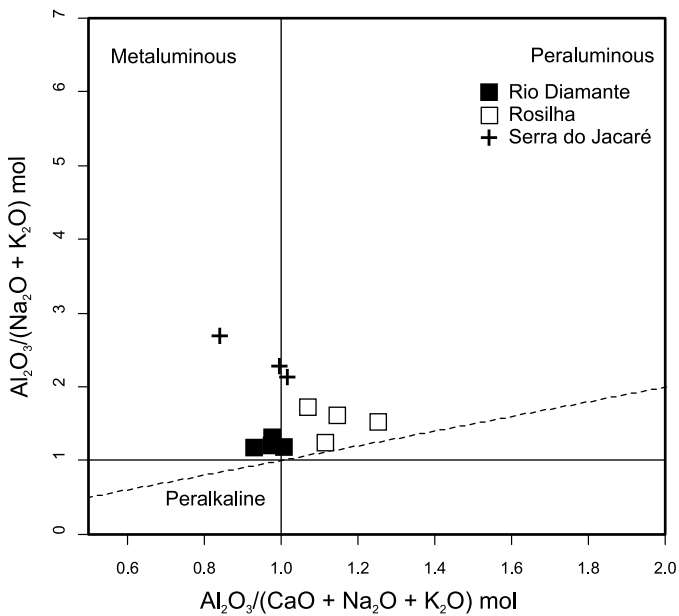
Fig. 11. SiO_2 versus K_2O diagram of Peccerilo and Taylor (1976) for volcanic rocks of the São Luís Craton.

environment, between the continental margin and the continent. This volcanic phase is coeval with the second, main volcanic arc stage.

7.4. A third volcanic stage?

Based on the equivocal geochronological data obtained for the Rosilha volcanic unit, we must also consider the possibility of a third volcanic event occurring at about 2068 Ma. This age difference might also explain the geochemical and isotopic differences found between the Rosilha and Rio Diamante volcanic rocks. Although uncommon in the São Luís Craton (only the Tracuateua Suite of 2086–2091 Ma was described so far, Palheta, 2001), ages in the 2060–2100 Ma range were recorded in several granite plutons that form part of the basement of the Gurupi Belt and are interpreted as related to a collision phase of a protracted (2240–2060 Ma) Paleoproterozoic orogenic event (Palheta, 2001; Klein et al., 2005a,b). However, recent dating (Klein et al., 2008) of a granite body spatially associated with the volcanic rocks studied here (Fig. 2) yielded ages between 2056 and 2076 Ma. This granite has been interpreted by Klein et al. (2008) as representing the post-orogenic stage in the evolution of the São Luís Craton. The characteristics presented by the Rosilha volcanic unit are consistent with this stage.
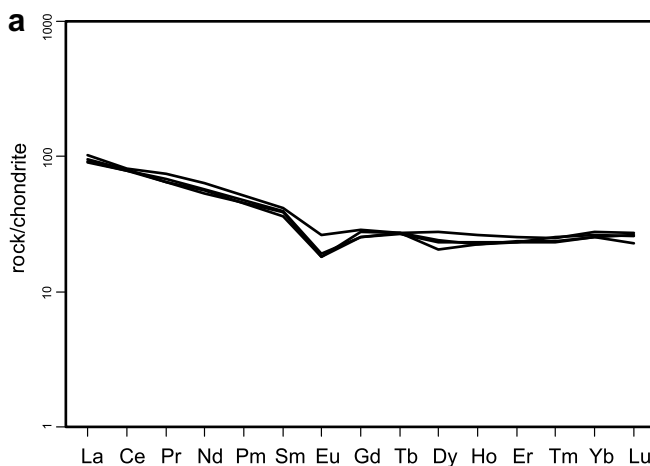
Fig. 12. (a) REE plot (normalized according to Boynton, 1984) and (b) trace element spidergram for volcanic rocks of the Rio Diamante Formation.
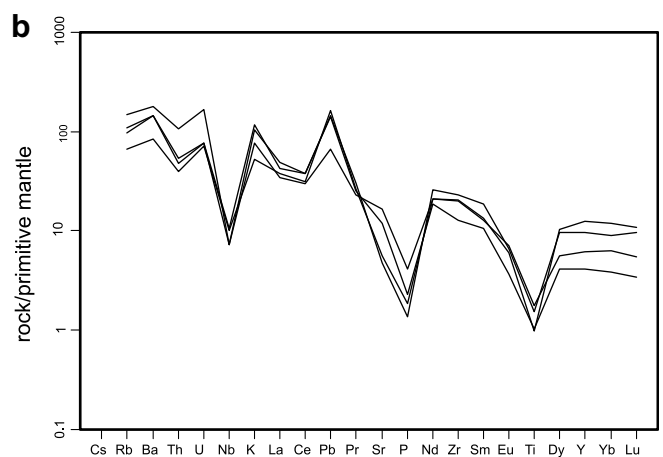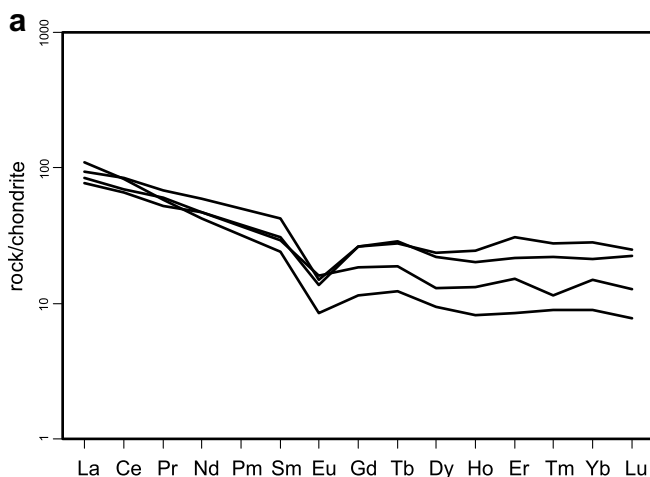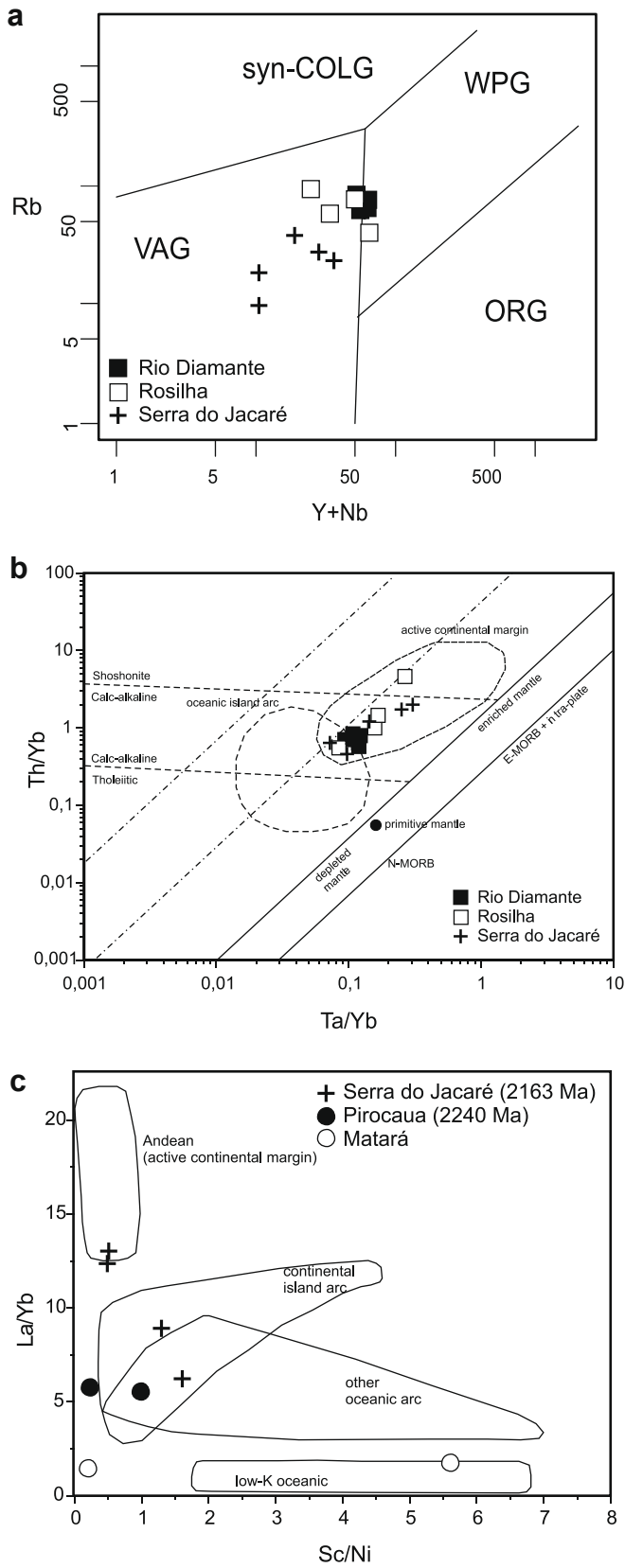

Fig. 13. (a) REE plot (normalized according to Boynton, 1984) and (b) trace element spidergram for samples of the Rosilha volcanic unit.

Fig. 14. Tectonic discrimination diagrams for acidic and intermediate volcanic and metavolcanic rocks of the São Luís Craton. (a) Rb × (Y + Nb) diagram of Pearce et al. (1984); (b) Th/Yb × Ta/Yb diagram combining the fields proposed by Pearce (1982) and Gorton and Schandl (2000); (c) La/Yb × Sc/Ni diagram for andesitic rocks (after Bailey, 1981).
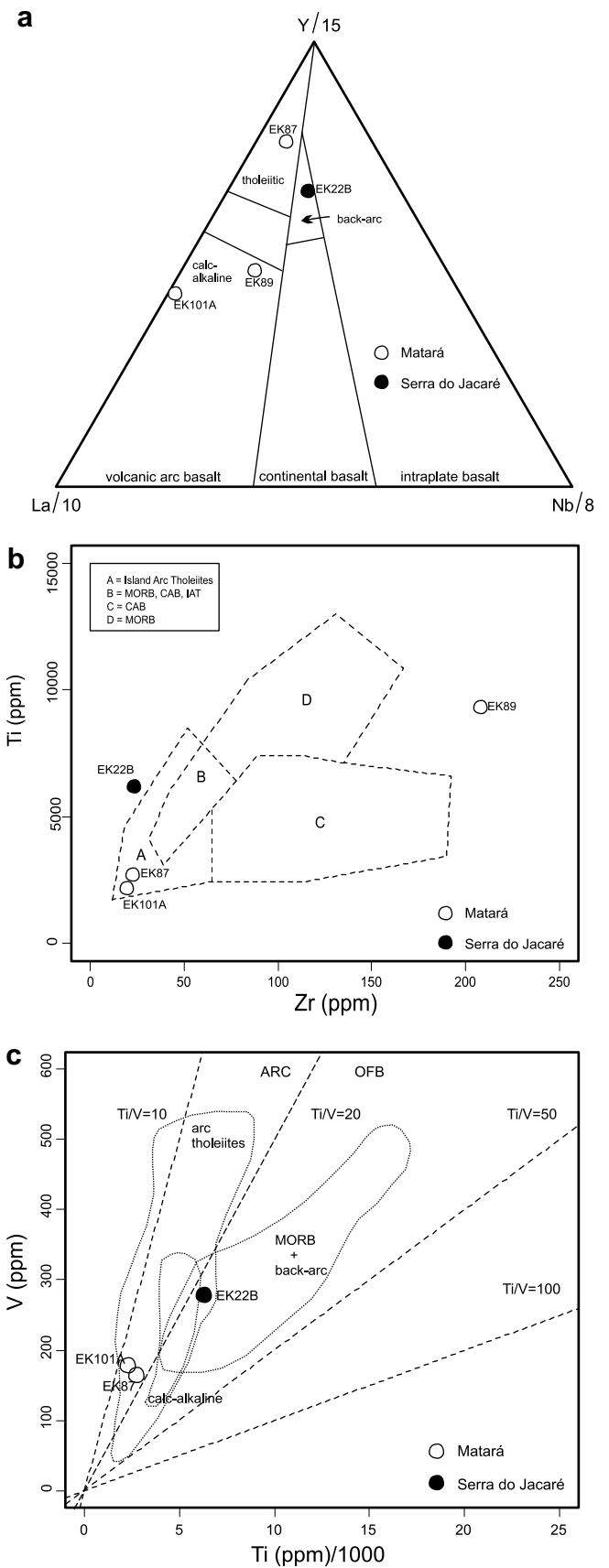
Fig. 15. Tectonic discrimination diagrams for basic volcanic and metavolcanic rocks of the São Luís Craton. (a) La/10–Y/15–Nb/8 diagram of Cabanis and Lecolle (1989); (b) Ti × Zr diagram of Pearce and Cann (1973); (c) V × Ti diagram of Shervais (1982).

8. Concluding remarks

The data presented in this paper bring new insights into the understanding of the magmatic and crustal evolution of the São Luís Craton. Three volcanic sequences have been described for the first time (Serra do Jacaré, Rio Diamante and Rosilha), and the understanding of the metavolcano-sedimentary Aurizona Group has been greatly improved. The metavolcanic rocks of the Aurizona Group are related to a volcanic arc (±back-arc) system. The Serra do Jacaré (mainly andesites and minor basaltic andesites) and Rio Diamante (dacites) formations likely define an active continental margin/continental arc or transition between a continental margin and the continent. These tectonic settings have not been recognized before, since the available data for granitoid rocks pointed out to intra-oceanic arc and collision settings. The tectonic meaning of the Rosilha unit (dacites) is still uncertain because of the lack of a precise age determination (2.16 Ga or 2.06 Ga). The two ages and the field and geochemical characteristics are consistent with both continental margin and post-orogenic settings.

In addition to a new understanding of the crustal evolution of the São Luís Craton the results obtained for the studied volcanic sequences bring continental and global-scale implications. The main implications are: (1) The São Luís Craton is composed predominantly of juvenile rocks formed between 2.20 and 2.15 Ga. However, especially for the volcanic sequences, the Nd evidence, some geochemical characteristics and inherited zircon crystals point to limited crustal reworking, mainly protoliths that experienced short crust residence time. (2) The period of juvenile accretion falls within the main period (2.2–2.0 Ga) of juvenile crust formation in the South American Platform (e.g., Cordani and Sato, 1999). (3) This period also correlates with the large production of juvenile crust in the West African Craton (e.g., Boher et al., 1992) and additionally supports the interpretation that considers the São Luís Craton as a fragment of that craton (Klein and Moura, 2008). (4) At least in part, the crust of the São Luís Craton formed between 2.4 and 2.2 Ga, which appears to be a period that experienced a growth rate of juvenile crust less than the background rate (Condie, 1997).

Conflict of interest statement

The author declares no relevant financial or other conflict of interest.

Acknowledgements

Appendix A. Summary of analytical procedures

U-Pb SHRIMP analyses were undertaken on SHRIMP II and RG of the Research School of Earth Sciences of the Australian National University, Canberra, Australia. Zircon crystals were hand-picked, mounted in epoxy resin, ground to half-thickness, and polished with diamond paste; a conductive gold-coating was applied just prior to analysis. SHRIMP analytical procedures followed the methods described in Compston et al. (1984) and Williams (1998). Raw data were reduced using the Squid program (Ludwig, 2001), and age calculations and concordia plots were done using both Squid and Isoplot/Ex software (Ludwig, 2003). Analyses for individual SHRIMP spots are plotted on concordia diagrams with 1σ uncertainties. Where data are combined to calculate an age, the quoted uncertainties are at 95% confidence level, with uncertainties in the U–Pb standard calibration included in any relevant U–Pb intercept and concordia age calculations.

Zircon dating by the Pb-evaporation method (Kober, 1986) was conduced at the Laboratório de Geologia Isotópica (Pará-Iso) of the Universidade Federal do Pará, Belém, using the double-filament array. Isotopic ratios were measured in a FINNIGAN MAT 262 mass spectrometer and data were acquired in the dynamic mode using the ion-counting system of the instrument. For each step of evaporation, a step age is calculated from the average of the $^{207}Pb/^{206}Pb$ ratios. When different steps yield similar ages, all are included in the calculation of the crystal age. If distinct crystals furnish similar mean ages, then a mean age is calculated for the sample. Crystals or steps showing lower ages probably reflect Pb loss after crystallization and are not included in sample age calculation. Common Pb corrections were made according to Stacey and Kramers (1975) and only blocks with $^{206}Pb/^{204}Pb$ ratios higher than 2500 were used for age calculations. $^{207}Pb/^{206}Pb$ ratios were corrected for mass fractionation by a factor of 0.12% per a.m.u, given by repeated analysis of the NBS-982 standard, and analytical uncertainties are given at the 2σ level.

Sm–Nd analyses were conduced at the Laboratório de Geocronologia of the Universidade de Brasília according to procedures described in Gioia and Pimentel (2000). Fifty milligram of whole rock powders were mixed with a $^{149}Sm/^{150}Nd$ spike and dissolved in Savilex vessels. The Sm–Nd separation used cation exchange Teflon columns with Ln–Spec resin, then Sm and Nd were deposited in Re filaments and the isotopic ratios were determined on a FINNIGAN MAT 262 mass spectrometer using the static mode. The Nd data were normalized to a $^{146}Nd/^{144}Nd$ ratio of 0.7219 and uncertainties in the Sm/Nd and $^{143}Nd/^{144}Nd$ ratios were about 0.4% (1σ) and 0.005% (1σ), respectively, based on repeated analysis of the BHVO-1 and BCR-1 standards. The crustal residence ages were calculated using the values of DePaolo (1988) for the depleted mantle (T_{DM}).

Major and trace elements were analyzed by ICP–ES and ICP–MS, respectively, at the Acme Analytical Laboratories Ltd. in Canada.

References

Abouchami, W., Boher, M., Michard, A., Albarede, F., 1990. A major 2.1 Ga event of mafic magmatism in West Africa: an early stage of crustal accretion. Journal of Geophysical Research 95 (B11), 17605–17629.

Abreu, F.A.M., Villas, R.N.N., Hasui, Y., 1980. Esboço estratigráfico do Precambriano da região do Gurupi; Estados do Pará e Maranhão. 31 Congresso Brasileiro de Geologia, Camboriú. pp. 647–658.

Bailey, J.C., 1981. Geochemical criteria for a refined tectonic discrimination of orogenic andesites. Chemical Geology, 139–154.

Boher, M., Abouchami, W., Michard, A., Albarède, F., Arndt, N., 1992. Crustal growth in West Africa at 2.1 Ga. Journal of Geophysical Research 97, 345–369.

Boynton, W.V., 1984. Cosmochemistry of the rare-earth elements: meteorite studies. In: Henderson, P. (Ed.), Rare-Earth Elements Geochemistry. Elsevier, Amsterdam, pp. 63–114.

Cabanis, B., Lecolle, M., 1989. Le diagramme La/10–Y/15–Nb/8: un outil pour la discrimination des series volcaniques et la mise en evidence des processus de mélange et/ou de contamination crustale. Comptes Rendus Academie des Sciences 309, 2023–2029.

Compston, W., Williams, I.S., Meyer, C., 1984. U–Pb geochronology of zircons from lunar breccia 73217 using a sensitive high-resolution ion-microprobe. Journal of Geophysical Research 98B, 525–534.

Condie, K.C., 1997. Plate Tectonics and Crustal Evolution. Butterworth-Heinemann, London. 282 p.

Cordani, U.G., Sato, K., 1999. Crustal evolution of the South American Platform, based on Nd isotopic systematics on granitoid rocks. Episodes 22, 167–173.

Costa, J.L., Araujo, A.A.F., Villas Boas, J.M., Faria, C.A.S., Silva Neto, C.S., Wanderley, V.J.R., 1977. Projeto Gurupi. Departamento Nacional da Produção Mineral/Companhia de Pesquisa de Recursos Minerai, 258.

Day, W.C., Aleinikoff, J.N., Gamble, B., 2000. Geochemistry and age constraints on metamorphism and deformation in the Fortymile river area, Eastern Yukon–Tanana Upland, Alaska. US Geological Survey Professional Paper, 1662.

DePaolo, D.J., 1988. Neodymium Isotope Geochemistry: An Introduction. Springer-Verlag, Berlin. 187 p.

Gioia, S.M.L.C., Pimentel, M.M., 2000. The Sm–Nd method in the geochronology laboratory of the University of Brasília. Anais da Academia Brasileira de Ciências 72, 219–245.

Gorton, M.P., Schandl, E.S., 2000. From continents to island arcs: a geochemical index of tectonic setting for arc-related and within-plate felsic to intermediate volcanic rocks. The Canadian Mineralogist 38, 1065–1073.

Hole, M.J., Saunders, A.D., Marriner, G.F., Tarney, J., 1984. Subduction of pelagic sediments: implications for the origin of Ce-anomalous basalts from the Mariana Islands. Journal of the Geological Society London 141, 453–472.

Klein, E.L., Moura, C.A.V., 2001. Age constraints on granitoids and metavolcanic rocks of the São Luís craton and Gurupi belt, northern Brazil: implications for lithostratigraphy and geological evolution. International Geology Review 43, 237–253.

Klein, E.L., Moura, C.A.V., 2003. Sintese geológica e geocronológica do Craton São Luís e do Cinturão Gurupi na região do rio Gurupi (NE-Para/NW-Maranhão). Revista Geologia USP, Série Científica 3, 97–112.

Klein, E.L., Moura, C.A.V., 2008. São Luís craton and Gurupi Belt (Brazil): possible links with the West African craton and surrounding Pan-African belts. In: Pankhurst, R.J., Trouw, R.A.J., Brito Neves, B.B., de Wit, M.J. (Eds.), West Gondwana: Pre-Cenozoic Correlations across the South Atlantic Region, vol. 294. Geological Society, London, Special Publications, pp. 137–151.

Klein, E.L., Moura, C.A.V., Krymsky, R., Griffin, W.L., 2005a. The Gurupi belt in northern Brazil: lithostratigraphy, geochronology, and geodynamic evolution. Precambrian Research 141, 83–105.

Klein, E.L., Moura, C.A.V., Pinheiro, B.L.S., 2005b. Paleoproterozoic crustal evolution of the São Luís Craton, Brazil: evidence from zircon geochronology and Sm–Nd isotopes. Gondwana Research 8, 177–186.

Klein, E.L., Larizzatti, J.H., Marinho, P.A.C., Rosa-Costa, L.T., Luzardo, R., Faraco, M.T.L., in press. Folha Cândido Mendes – SA.23-V-D-II, Estado do Maranhão, Escala 1:100.000. Geologia e Recursos Minerais. Companhia de Pesquisa de Recursos Minerais/Serviço Geológico do Brasil.

Klein, E.L., Luzardo, R., Moura, C.A.V., Armstrong, R., 2008. Geochemistry and zircon geochronology of Paleoproterozoic granitoids: further evidence on the magmatic and crustal evolution of the São Luís Craton, Brazil. Precambrian Research, in press.

Kober, B., 1986. Whole-grain evaporation for 207Pb/206Pb-age-investigations on single zircons using a double-filament source. Contributions to Mineralogy and Petrology 93, 482–490.

Ludden, J.N., Thompson, G., 1979. An evaluation of the behaviour of the rare earth elements during the weathering of sea-floor basalt. Earth Planetary Science Letters 43, 85–92.

Ludwig, K.R., 2001. Squid version 1.03 – A user's manual. Berkeley Geochronology Center Special Publication, vol. 2, 18 p.

Ludwig, K.R., 2003. User's manual for Isoplot/Ex version 3.00 – A geochronology toolkit for Microsoft Excel. Berkeley Geochronological Center Special Publication, vol. 4, 70 p.

Palheta, E.S.M., 2001. Evolução geológica da região nordeste do Estado do Pará com base em estudos estruturais e isotópicos de granitóides. Unpub. MSc Thesis, Universidade Federal do Pará, Belém.

Pastana, J.M.N., 1995. Programa Levantamentos Geológicos Básicos do Brasil. Programa Grande Carajás. Turiaçu/Pinheiro, folhas SA.23-V-D/SA.23-Y-B. Estados do Pará e Maranhão. Brasília, Companhia de Pesquisa de Recursos Minerais, 205.

Pearce, J.A., 1982. Trace element characteristics of lavas from destructive plate boundaries. In: Thorpe, R.S. (Ed.), Andesites. Wiley, Chichester, pp. 525–548.

Pearce, J.A., Cann, J.R., 1973. Tectonic setting of basic volcanic rocks determined using trace element analyses. Earth Planetary Science Letters 19, 290–300.

Pearce, J.A., Harris, N.B.W., Tindle, A.G., 1984. Trace element discrimination diagrams for the tectonic interpretation of granitic rocks. Journal of Petrology 25, 956–983.

Peccerilo, A., Taylor, S.R., 1976. Geochemistry of Eocene calc-alkaline volcanic rocks from the Kastamonu area, northern Turkey. Journal of Petrology 58, 63–81.

Poujol, M., Kiefer, R., Robb, L.J., Anhaeusser, C.R., Armstrong, R.A., 2005. New U–Pb data on zircons from the Amalia greenstone belt, Southern Africa: insights into the Neoarchaean evolution of the Kaapvaal Craton. South African Journal of Geology 108, 317–332.

Rollinson, H.R., 1993. Using geochemical data: evaluation, presentation, interpretation. Longman, New York. 352 p..

Shervais, J.W., 1982. Ti–V plots and the petrogenesis of modern and ophiolitic lavas. Earth and Planetary Science Letters 59, 101–118.

Shimizu, H., Sawatari, H., Kawata, Y., Dunkleu, P.N., Masuda, A., 1992. Ce and Nd isotope geochemistry on island arc volcanic rocks with negative Ce anomaly: existence of sources with concave REE patterns in the mantle beneath the Solomon and Bonin island arcs. Contributions to Mineralogy and Petrology 110, 242–252.

Stacey, J.S., Kramers, J.D., 1975. Approximation of terrestrial lead isotope evolution by a two-stage model. Earth Planetary Science Letters 26, 207–221.

Sylvester, P.J., Attoh, K., 1992. Lithostratigraphy and composition of 2.1 Ga greenstone belts of the West African Craton and their bearing on crustal evolution and the Archean-Proterozoic boundary. Journal of Geology 100, 377–393.

Vanderhaeghe, O., Ledru, D., Thiéblemont, D., Egal, E., Cocherie, A., Tegyey, M., Milési, J.P., 1998. Contrasting mechanisms of crustal growth. Geodynamic evolution of the Paleoproterozoic granite-greenstone belts of French Guiana. Precambrian Research 92, 165–193.

Watters, B.R., Pearce, J.A., 1987. Metavolcanic rocks of the La Ronge Domain in the Churchill Province, Saskatchewan: geochemical evidence for a volcanic arc origin. In: Pharaoh, T.C., Beckinsale, R.D., Rickard, D. (Eds.), Geochemistry and mineralization of Proterozoic volcanic suites, 33. Geological Society Special Publications, pp. 167–182.

Williams, I.S., 1998. U–Th–Pb geochronology by ion microprobe. In: McKibben, M.A., , Shanks, W.C., III, Ridley, W.I. (Eds.), Applications of microanalytical techniques to understanding mineralizing processes, 7. Reviews in Economic Geology, pp. 1–35.

Wilson, M., 1989. Igneous petrogenesis. A Global Tectonic Approach. Chapman & Hall, London. p. 466.

Winchester, J.A., Floyd, P.A., 1977. Geochemical discrimination of different magma series and their differentiation products using immobile elements. Chemical Geology 20, 325–343.

Winter, J.D., 2001. Introduction to Igneous and Metamorphic Petrology. Prentice Hall, New Jersey 697 p.